8-7-91

CONTRACTOR REPORT

SAND91—7009
Unlimited Release
UC—237

Facet Development for a Faceted Stretched-Membrane Dish by Solar Kinetics, Inc.

P.T. Schertz, P. E., D. C. Brown, A. Konnerth III

Solar Kinetics, Inc.
10635 King William Dr.
Dallas, TX 75220

Prepared by Sandia National Laboratories Albuquerque New Mexico 87185 and Livermore California 94550 for the United States Department of Energy under Contract DE AC04 76DP00789

Printed July 1991

Issued by Sandia National Laboratories, operated for the United States Department of Energy by Sandia Corporation.

Available to DOE and DOE contractors from
Office of Scientific and Technical Information
PO Box 62
Oak Ridge, TN 37831

Prices available from (615) 576-8401, FTS 626-8401

Available to the public from
National Technical Information Service
US Department of Commerce
5285 Port Royal Rd
Springfield, VA 22161

NTIS price codes
Printed copy: A05
Microfiche copy: A01

SAND--91-7009

DE91 016866

SAND91-7009
Unlimited Release
Printed July 1991

FACET DEVELOPMENT FOR A FACETED STRETCHED-MEMBRANE DISH BY SOLAR KINETICS, INC.

P. T. Schertz, P.E.
D.C. Brown
A. Konnerth III

Solar Kinetics, Inc.
10635 King William Drive
Dallas, TX 75220

Sandia Contract: 42-9814B

ABSTRACT

A 3.6-meter diameter stretched-membrane optical facet for a parabolic dish has been successfully designed and demonstrated under contract with Sandia National Laboratories. Twelve facets identical to them will be used to make the lightweight reflector of the dish. The project goal of 2.5-mrad surface accuracy was met with each of the two full-sized prototypes, and accuracies of as low as 1.1 mrad were achieved. The facet weight is 11.7 kg/m^2 (2.4lbs/ft^2).

The facet is similar in construction to the successful stretched-membrane heliostat; it has two thin metal membranes attached to a ring. However, the front membrane for this facet is plastically formed at the factory in order to achieve a shorter facet f/D (approximately 3.0). A passive tether restrains the front membrane when not in operation, that is, when the stabilizing vacuum is off. The optical surface is achieved with a silvered-acrylic film laminated to the metal membrane. The facet is expected to cost \$55.40/m^2 at a production rate of 10,000 facets per year and \$115,000/m^2 at a production rate of 500 facets a year.

Several key issues have been resolved. Stress concentrations due to seams in the reflective laminate did not cause membrane rupture during forming as they have for dishes with lower focal length-to-diameter ratios. The laminate survived the forming process and simulated operation without deterioration. The optical effect of the tether on the membrane was tested and found to be very small. Most important, highly accurate shapes were obtained using a simple forming procedure. Additional tests are needed to demonstrate process repeatablilily and facet performance in typical operating conditions.

Contents

List of Figures

List of Tables

1.0 INTRODUCTION

Solar Kinetics, Inc. (SKI) has successfully designed and demonstrated a stretched-membrane optical facet under contract to Sandia National Laboratories. Twelve of these identical facets are to be used on a faceted dish for a 25 kW_e dish-Stirling system.

Sandia is developing a solar concentrator for the Department of Energy's Solar Thermal program. This dish is intended to result in a low risk, near-term implementation of a concentrator by building on advances made in stretched-membrane heliostat development. This concentrator will be integrated with an advanced solar receiver and a Stirling engine/generator in a 25 kW_e modular, power production unit. The faceted membrane approach is being pursued as an alternative to the higher risk single-element dish and more costly glass/metal dishes.

Concurrent with SKI's effort, Science Applications International Corporation (SAIC) developed an alternative facet and WGAssociates designed the dish structure and drive. Sandia and the Solar Energy Research Institute (SERI) actively participated in this effort. SERI performed detailed optical evaluation of the facets and has performed stress tests of membrane material. Sandia provided management and analysis and is currently testing the facets at the National Solar Thermal Test Facility.

The SKI facet is similar in appearance to stretched-membrane heliostats in that two membranes are supported from a ring, and a partial vacuum induced in the enclosed volume between the membranes focuses the optical surface. Unlike the heliostats, the front membrane is plastically formed to a concave shape. This departure from the heliostat concept was selected to achieve the goals of low weight and high optical quality. The facet weighs only 11.7 kg/m^2 (2.4 lbs/ft^2) and reached an optical accuracy of 1.1 mrad. The front membrane of the facet is tethered to the rear membrane as shown in Figure 1.1. This tether induces a load in the front membrane that stabilizes it when there is no focusing vacuum. The tether is passively activated and disengages when the vacuum is reapplied.

This report documents SKI's effort in the first of two planned phases. The following section of this report describes the rationale behind the decision to plastically form the facet. The next six sections provide a detailed description of the design process for each of the major facet components. A cost analysis for commercial facet production is provided in Section 9. Section 10 describes the successful construction and demonstration of the prototypes.

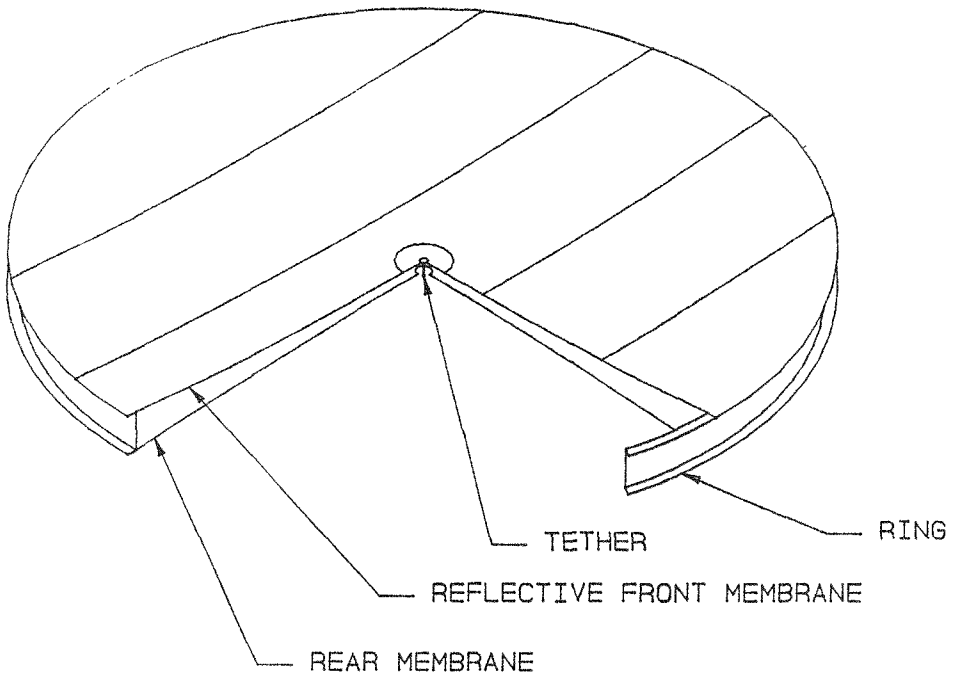

Figure 1.1 Facet Description

2.0 CONCEPT SELECTION

The concept of plastically forming the facet's front membrane significantly departs from the convention of stretched-membrane heliostats. Although this facet concept was selected during the proposal phase of the contract, its selection warrants discussion because of its departure from convention.

The two concepts seriously considered by SKI were the heliostat concept having two membranes that remained elastic and the plastic concept having the reflective membrane plastically formed (yielded) during manufacturing. Other variations were briefly considered but rejected because of unacceptably high development risks. The heliostat approach has the advantage of simplicity; two membranes are stretched on a ring and kept in the elastic range. However, this approach had four significant disadvantages: high membrane stress, high operational pressure, high ring weight, and potential limitations on performance.

A membrane that is initially flat and elastically pulled to a short f/D would be subjected to high stresses. Figure 2.1 shows this relation for stainless steel having no initial tension (based on method presented by Murphy, Ref. 1). The minimum f/D of interest was 2.2 which has a stress level of 640 MPa (93,000 psi). Initial tension would increase the stress. Membrane thickness has no affect on stress levels. Typical yield strengths for annealed stainless steel are 200 to 280 MPa (30,000 to 40,000 psi). Cold worked or tempered stainless has a higher yield strength, but uncertainties would be created with regard to change of properties in the weld zones and decreased material ductility. This could increase the chance of rupture due to local imperfections.

The minimum operational pressure for the elastic concept is defined by the mechanical resistance of the membrane to deflection. Figure 2.2 shows the pressure required to elastically deform a 0.08 mm (3 mil) thick stainless membrane assuming no initial tension (Ref. 1). Initial tension would increase the pressure requirements. The pressure requirements for stretched-membrane heliostats and single-element dishes are also shown in Figure 2.2 for comparison. One effect of high operational pressure is the parasitic power consumption required to maintain the pressure. The plastically formed concept does not have this limitation. Pressure requirements for the plastic approach are largely defined by dynamic pressure fluctuations of the wind and are much lower than the elastic approach (the selected range is also shown in the figure).

The most significant load in the ring is caused by the membranes. The elastic concept suffers from high ring loads that results in high ring weight. Figure 2.3 shows the compressive ring load caused by the membranes. It was assumed that the front and rear membranes were 0.08 mm (3 mil) thick stainless steel installed with no pretension and subjected to the load of the operational vacuum only. Pretension or thicker membranes would increase the ring load. (Membrane imposed ring loads for elastic membranes were based on relations presented in Ref. 1) Data for plastically formed membranes are also presented in Figure 2.3 for comparison. Properties of the final

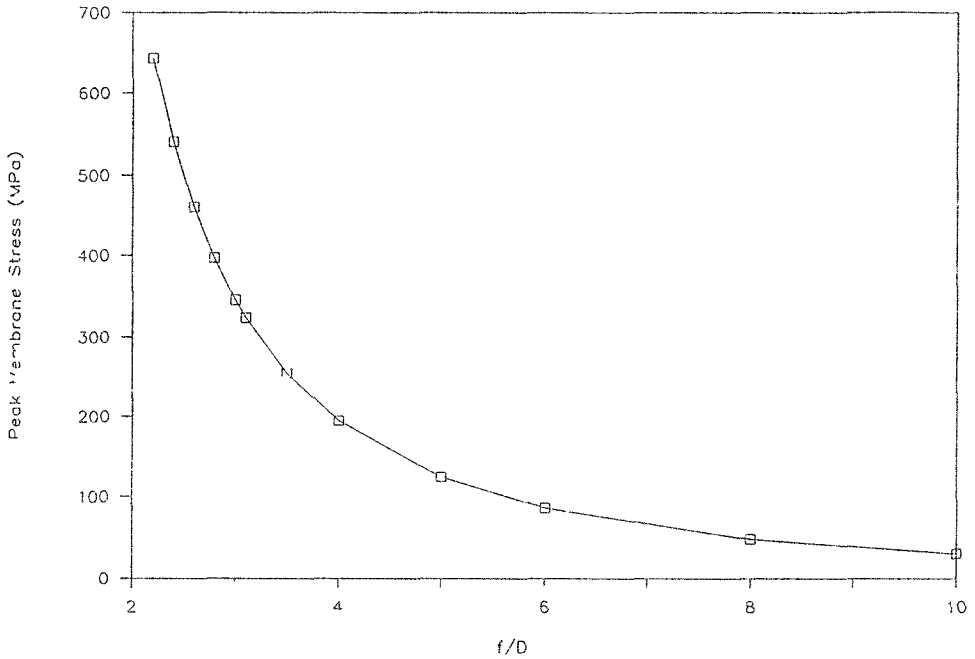

Figure 2.1 Membrane Stress for the Elastic Membrane Concept.

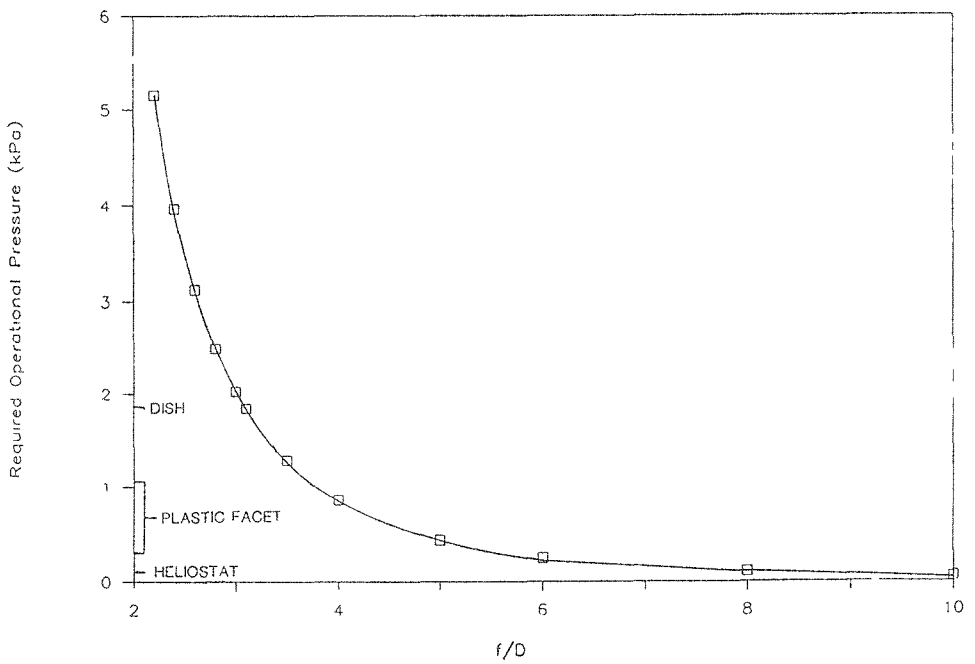

Figure 2.2 Minimum Operational Pressure for the Elastic Membrane Concept.

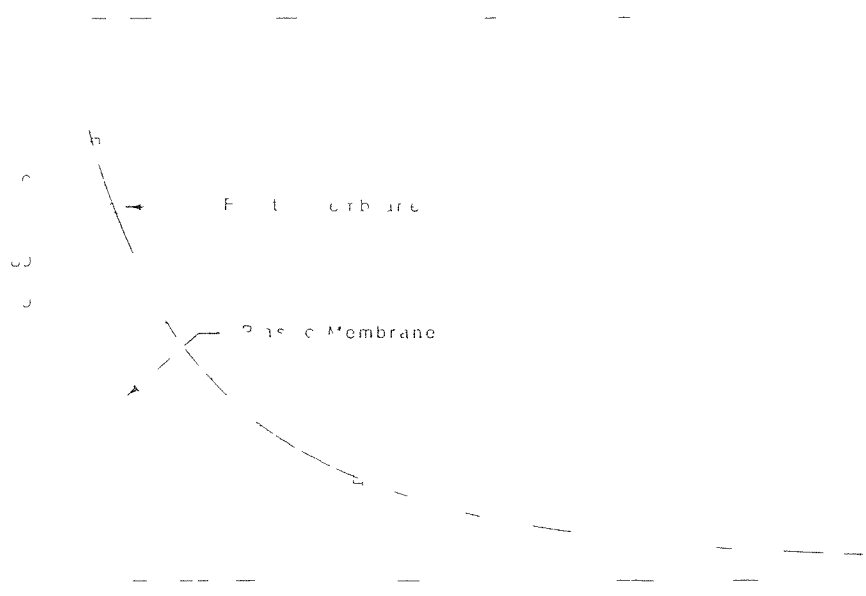

Figure 2.3 Compressive Ring Load for the Elastic Membrane Concept.

facet design were used to generate this curve. That is, it was assumed that the front membrane was formed and the rear membrane was elastic. A 0.10 mm (4 mil) rear stainless steel membrane with an initial tension of 5300 N/m (30 lbs/in) was used with a 0.08 mm (3 mil) stainless steel front membrane. The vacuum levels were those measured for the second prototype facet. The use of high strength ring material does not mitigate the effect of high ring loads because the tall thin ring sections are limited by local buckling for which wall thickness and material modulus are the key properties. The significance of this is that the ring for the elastic membrane approach must be heavier than that used for the plastic approach.

Finally, the elastic membrane response of the heliostat approach could limit the optical quality of the membrane. Murphy has stated that good shapes "can be obtained with totally elastic membrane systems if f/D is greater than 2.0 and if (Et/T_0) is small...if (Et/T_0) is large, the required f/D for acceptable surface contours may grow appreciably above 2.0" where E is the membrane material modulus of elasticity, t is the material thickness, and T_0 is the initial membrane tension (Ref. 2). To improve (Et/T_0), the designer is forced to increase the initial tension. Membrane thickness is restricted by field durability, and membrane modulus is constrained by material yield strength concerns. Increases in initial membrane tension to improve the optical contour would be detrimental in that it would increase membrane stress, increase operational pressure, and increase ring weight.

At the start of the project, the plastic concept was not without disadvantages. The shape that could be obtained from plastically forming membranes with uniform pressure was an unknown. It was not known if a tether could be implemented without complexities and damage to the front membrane. It was also not known if the silver polymer film could survive the high strains of the forming process. These uncertainties were resolved early in the project by testing of membranes on an existing tooling ring. SKI felt that it was better to accept these uncertainties than suffer the uncertainties of the elastic approach, and most significantly, be burdened with its inherent limitations.

The remaining disadvantages of the plastic concept is the additional manufacturing step required to form the membrane and the cost of the tether. The cost of forming is not trivial for prototypes and small-volume production, but becomes insignificant with higher production rates. The cost of the tether is relatively small, at approximately 2% of the facet cost.

The contract design specifications for the facet f/D were changed after initiation of the contract. This change improved the merit of both concepts. The original specification called for a variable f/D from 2.2 to 3.1 and was later changed to 2.7 to 3.0. This change benefited the plastic concept in that only one facet type would be needed for the entire range. Three or four types of facets would be required for the original f/D range, each having a membrane formed to a different focal length. This would have increased the complexity of manufacturing and increased the cost accordingly. The specification change benefitted the elastic membrane concept by reducing the membrane stress (34%), reducing operational pressure (47%), reducing ring load (34%), and reducing optical errors caused by small f/D's. This specification change altered the relative merit of the two concepts, but did not eliminate the disadvantages of the elastic approach and did not warrant switching concepts.

3.0 MEMBRANE TESTS

Several tests were performed early in the project to resolve fundamental issues associated with plastically formed membranes. These tests demonstrated: that acceptable membrane contours could be achieved; that the polymer film did not induce rupture in the metal membrane during forming and showed no signs of failure itself; and that a passive tether would not damage the membrane.

The membrane forming tests involved forming and artificially tethering a 3.7-m membrane on an existing tooling ring. An oversized membrane was clamped to a rigid tooling ring as shown in Figure 3.1. A partial vacuum was drawn on the plenum to plastically yield and form the membrane. The shape of the formed membrane was measured with a set of two dial indicators mounted in parallel 12.7 cm (5 inches) apart. The dial indicators measured the relative displacement of two points on the membrane from which slope was calculated. Slope measurements were taken at ten locations along diametral lines. At each measurement location the jig holding the indicators was precisely leveled prior to making measurements. The accuracy of this unit was measured using a sine bar to +/- 0.3 mrad. The actual accuracy is slightly worse because of the local distortions of the membrane caused by the pressure of the dial indicators. The repeatability of the measurement was checked by scanning a membrane twice under identical conditions. Figure 3.2 shows the results of this scan. The RMS repeatability was found to be 0.2 mrad.

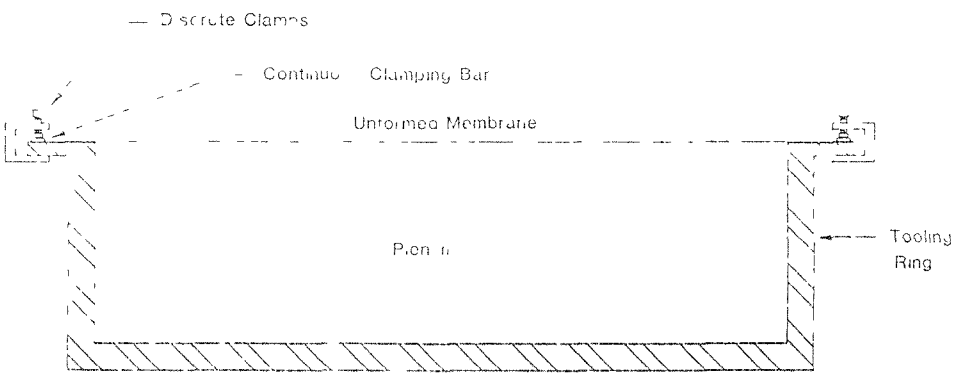

Figure 3.1 Tooling Used for Membrane Tests.

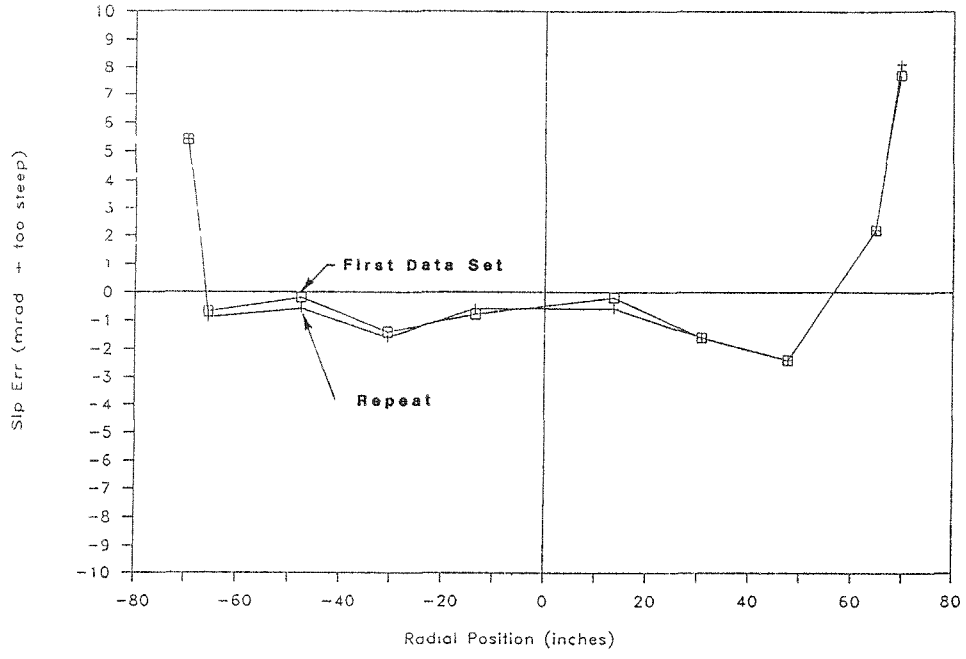

Figure 3.2 Repeatability Test of Slope Measurement Technique.

The membrane material used for the test was 304 annealed stainless steel, 0.08 mm (3 mils) thick made from 0.91 m (36 inch) wide coil stock. ECP-305 was laminated to the stainless steel using a dry, pinch roll process. The steel sheets were joined along their edges with a 12 mm (0.5 inch) lap joint with two rows of discrete electric resistance spot welds. The row spacing was 6 mm (0.25 inches). The upper free edge of the lap joint was tacked on 25 mm (one inch) spacing with an electric resistance spot welder. This is the same material and technique used for the prototype facets.

Uniform pressure was used to plastically yield and form the membrane. The forming pressure was incrementally increased. After each increase, the pressure was reduced to 345 Pa (0.05 psi), which is the operational pressure desired for an f/D of 3.0, and then the center deflection was measured. Forming was stopped when the center deflection reached that of a parabola with an f/D of 3.0.

Figure 3.3 shows the measured slope error of this membrane for scans parallel and perpendicular to the seams. During measurement the membrane was under 345 Pa (0.05 psi) stabilization pressure. Slope error is defined as the difference between the measured slope and that of a perfect parabola having a center deflection the same as what was measured. With only ten data points per scan, no meaningful single value can be calculated to express the slope error of the membrane (such as an RMS area weighted error). However, the low error terms at the ten measured locations were sufficient for us to determine that the forming process was acceptable.

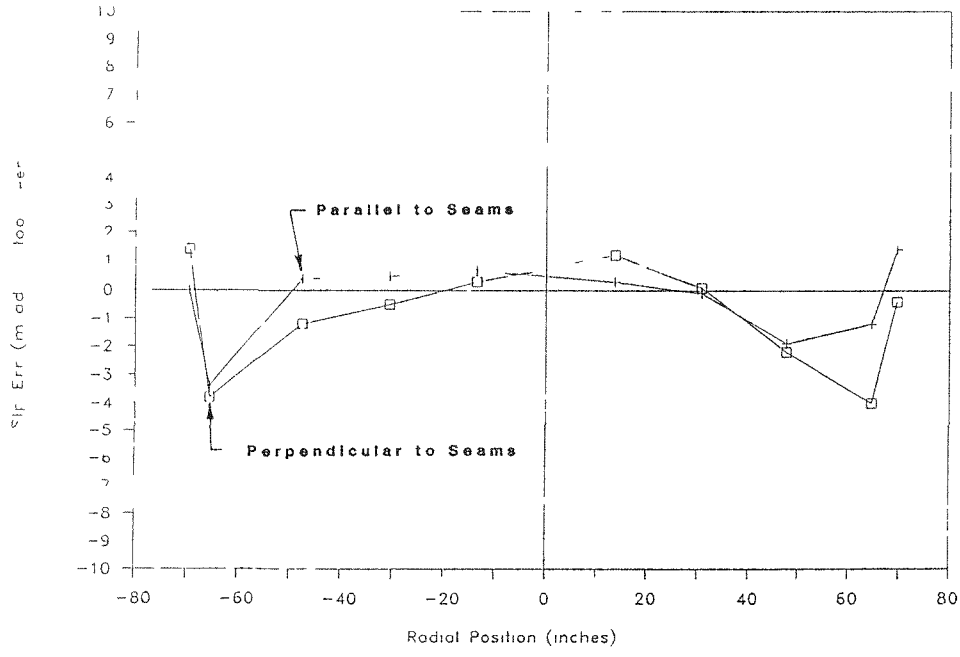

Figure 3.3 Slope Error with Respect to Seams for a Membrane Test.

Shorter facet focal lengths than the formed 3.0 f/D are obtained by reducing the vacuum pressure in the plenum. No further forming was done on this test membrane or on the facets. Figure 3.4 shows the slope error for four different focal lengths or f/D's. The error changes little except for the outer portion of the membrane. Although this effect was not encouraging, it does not seem to be so large that the technique is unacceptable.

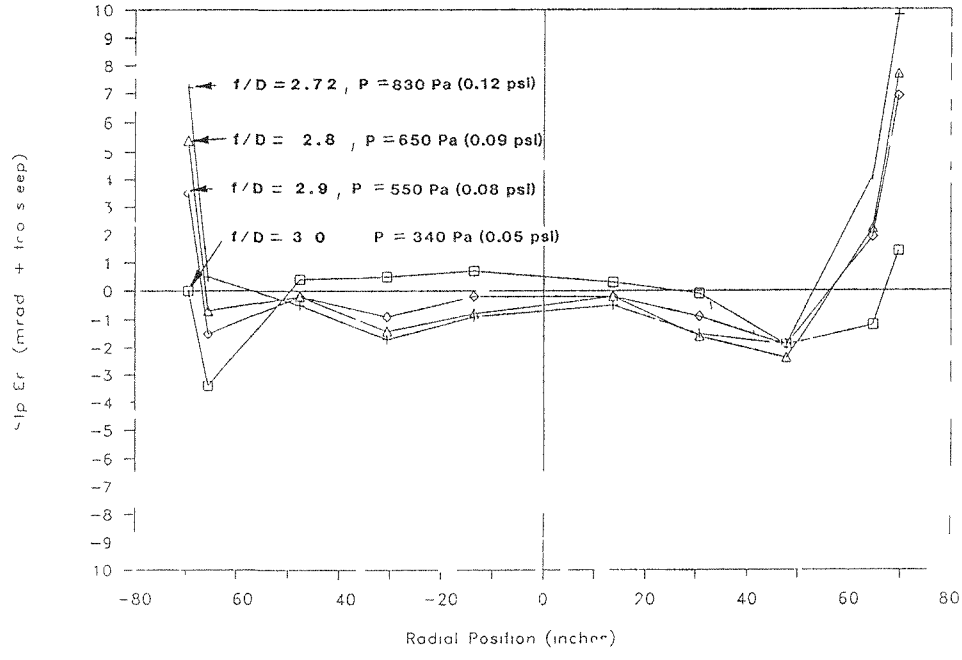

Figure 3.4 Effect of Focal Length Change on a Test Membrane.

During work with single element stretched-membrane dishes, SKI formed metal membranes laminated with ECP-300 (Ref. 3). The joints in the ECP caused stress concentrations in the metal. The metal deformation became localized, and the metal membranes ruptured. The magnitude of strain required for forming multifaceted dish membranes is considerably less than for the single element dish. The membrane forming test demonstrated that the strain was within the range acceptable for the forming process. The membrane did not rupture and no cracking or crazing of the ECP-305 polymer film was observed.

A test was done with this membrane to evaluate the effects of tethering the front membrane. This tether induces a load at the center of each membrane that pulls them closer together. The magnitude of the load is dependent on wind conditions and on the stiffness of the rear membrane. The artificial tether was a rounded disk having an area of contact similar to that of the final design (140 cm^2 or 22 in^2). It was held against the membrane with a hydraulic cylinder as shown in Figure 3.5. Air was added to the plenum to create a positive pressure to simulate a rear wind on the facet. The tether was raised as the pressure was increased. This was done to model the effect of the rear membrane (and tether restraint) moving forward under the combined loads of the wind and the tether. The relationship of this load and deflection was not known at the time of the test because the rear membrane configuration had not been defined. A set of reasonably harsh conditions was selected to establish whether or not the membrane was sensitive to the tether.

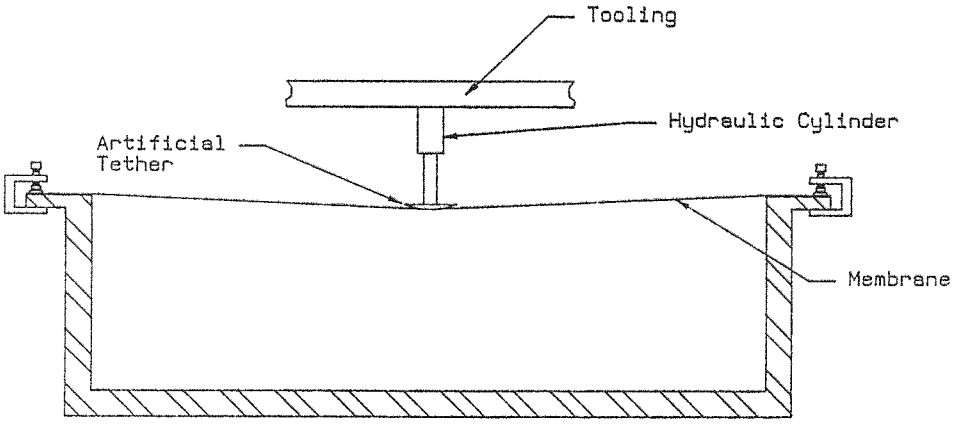

Figure 3.5 Tether Test Schematic.

The artificial tether was initially pushed into the membrane with a force of 155 N (35 pounds) with no pressure or vacuum in the plenum. The tether position was then held constant, and the plenum pressure increased to 27 Pa (0.004 psi). The resulting force on the tether was 440 N (100 pounds). The tether was then raised 60 mm (2.4 inches), and the pressure was increased to 76 Pa (0.011 psi). The resulting tether force was 380 N (85 pounds). The tether was allowed to rise another inch so that the center of the membrane was 13 mm (0.5 inches) above the ring plane, and the plenum pressure was increased to 150 Pa (0.022 psi). The resulting tether force was 490 N (110 pounds). The load was removed, and the membrane was inspected after each increase of pressure. No membrane damage was visible. The contour was measured following this test. A before and after comparison is presented in Figure 3.6. No significant changes are evident near the region of the tether. It is important to note that very localized errors would not be resolved with the measurement technique used. We relied on visual inspection to detect local errors.

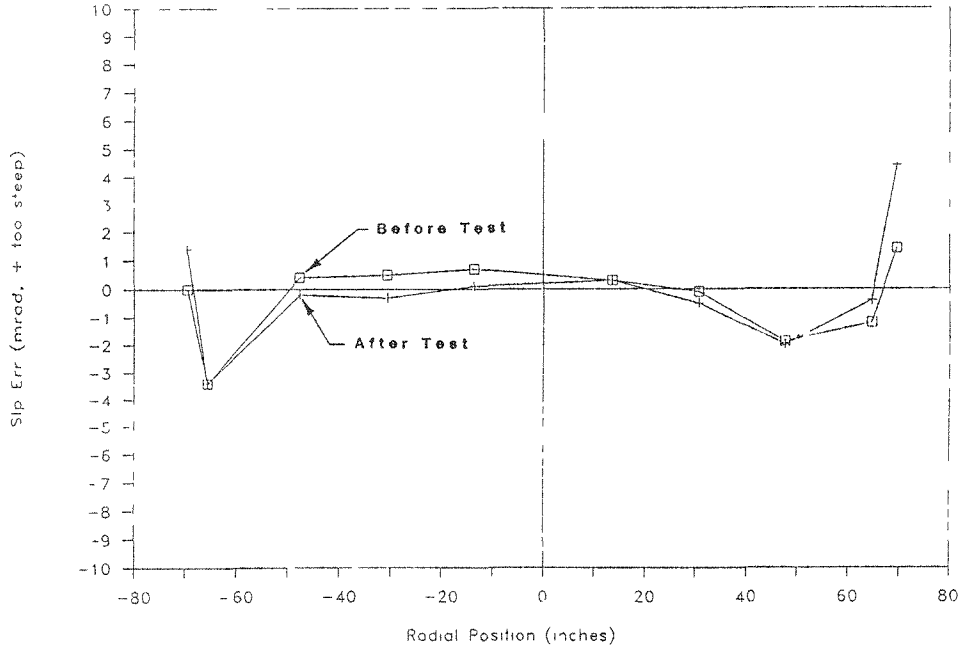

Figure 3.6 Effect of Tether on Test Membrane.

4.0 MEMBRANE AND TETHER DESIGN

The design of the membranes and tether and the selection of the operational vacuum for the facet are closely related and are discussed in this section.

4.1 OPERATIONAL PRESSURE

Each facet on a dish has the same design, and their membranes will be formed the same. They will be formed such that a predefined minimum operational pressure will create the long focal length (10.5 m). Shorter focal lengths would be obtained by increasing the vacuum. The minimum operational pressure was set high enough so that wind gusts would not significantly alter the shape of the facet. (The short duration of wind gusts makes it impractical for a control system to respond to them.) The minimum operational pressure was arbitrarily selected early in the design effort to 340 Pa (0.05 psi). The appropriateness of this selection was later confirmed, and no design iterations were required. This sequencing was required because the passive response of the facet is a function of its structural design, which is influenced by the loading imposed by the operational pressure.

The maximum operational wind speed (including gust) adopted for this contract is 12 m/s (27 mph) with a gust factor of 1.6 (Ref. 4). The gust factor is the ratio of peak wind speed (mean plus gust) to mean wind speed. This, then defines the magnitude of the gust or the transient wind pressure.

The pressure from a wind gust is carried by both facet membranes. The load each membrane carries is a function of their relative stiffness (this has been demonstrated with stretched-membrane heliostats, Ref. 5). The front and rear membranes have approximately equal stiffness under operating conditions, therefore, they share the wind load equally. The resulting membrane deflection as a result of the wind gust is half that of the front membrane if it were exposed to the full force of the wind. The resulting slope error is approximately 0.8 mrad based on measured response of the first facet to changes in pressure.

This was judged to be acceptable based on the following considerations:

1) This would be a rare occurrence happening only when the wind peaks to 27 mph during operation. At lower wind speeds, the error would be much smaller because the wind pressure is a function of the square of the wind speed.

2) This analysis assumed the facet faced directly into the wind. All facets of a dish cannot simultaneously face the wind, therefore, the dish error would be less. Also, the probability of the dish facing the horizon into the wind when a 27 mph gust arrives is low.

3) The membrane will oscillate with the changing gust pressures. The time averaged error would be less.

The effect of the focal point moving in and out of the receiver is not expected to be a problem with respect to receiver damage because of its short dwell times. The dwell times would closely follow the gust durations and are site specific.

4.2 FRONT MEMBRANE

Stainless steel membranes were proposed for this project because they are ductile and easily formed. The 304 alloy was selected because of its good atmospheric corrosion resistance and because it maintains ductility in the weld region. A thickness of 0.08 mm (3 mil) was selected for the front membrane based on demonstrated hail resistance in similar applications (Ref. 6). Membrane yield does not limit the thickness because yielding would occur with a pressure differential of 2400 Pa (0.35 psi), and the peak differential is expected to be 1500 Pa (0.22 psi). The membrane is laminated with reflective film per contract specifications. The selected film was ECP-305 based on its high specular reflectivity and known weatherability.

SERI cycle tested front membrane material samples and found no ill effects. The laminated material was plastically yielded to 0.1% elongation and then cycled between 0 and 0.04% additional strain corresponding with membrane forming and operation. This was done with uniaxial stress. A load of 6700 N/m (38 lbs/in) was applied during 2880 cycles. Cycle time was approximately one minute. Visual inspection showed no defects and 250X microscopy revealed no adverse impact on the polymer or silver (Ref. 7).

SERI has shown with laboratory samples that ECP silver corrosion is reduced if the substrate is painted. A review was done to determine if any manufacturing restrictions exist with respect to the use of coil-coated membranes. This issue was discussed with several companies that do coil-coating. No company was found that was able to coat material as thin as 0.08 mm (3 mil) in a coil process. Their machines are designed for heavier stock (typically 0.46 mm (18 mil) and above) and have difficulty guiding thin material.

Coil-coating lines are long and elaborate. They must clean, coat, bake, and recoil the material. A significant amount of material is dedicated (lost) just to initially feeding the material through the line. This drives up the cost for small runs. SKI was unable to find a coil-coater interested in coating as little as 1600 kg (3500 pounds) (enough material for 250 facets). Typical orders are 18,000 kg (40,000 pounds) (3000 facets).

Welding of material would be complicated if it was painted in the weld area. This can be avoided by a "striping" process where the coil is coated over only part of its width. This seems to be a common process that would also avoid the cost of painting the rear surfaces of the sheet.

SKI has pursued coil-coated steel for a mass-production study of parabolic troughs. The material was considerably thicker than that used for the membranes, so coating system compatibility was not a problem. Considerable effort was required to obtain a

painted finish that did not reduce the specularity of the laminated ECP. Although this problem was resolved, it illustrated a sensitivity that would have to be considered if a dish manufacturer were to develop a small-scale painting operation for coating thin membranes.

The benefit of using painted stock did not outweigh the development costs and uncertainty of its use. Bare stainless steel was selected as the substrate material.

The angle of departure of the membrane to the ring is approximately five degrees during operation and stow. When a strong wind acts on the tethered membrane from the rear, the angle of departure could change from roughly five degrees to less than zero. The bending stress in the membrane from this action is considerable and the potential for fatigue failure exists. The stress can be reduced by having the membrane depart from the ring over a large radius. The roll-formed ring now provides a radius of 0.25 inches. A plastic part was designed to provide a larger radius. This part was not included in the final design because it may not be needed. The cost and complexities of the part were not warranted in light of the uncertainty of the magnitude of the tethered membrane's reaction to wind. The part can be included in the design if testing shows that the membrane cycles to this magnitude repeatedly.

4.3 PASSIVE TETHER

The thin, contoured front membrane is not stable in the wind unless restrained. If unrestrained, the membrane would flutter and could destroy itself. Pressure provides stability during operation. During nonoperating periods, the membrane is restrained mechanically with a tether that pulls the center of the front membrane toward the rear membrane. This induces radial tension in the front membrane that makes the membrane resistant to flutter.

The tether is inactive during facet operation and induces no force on the membrane. Its operation is shown in Figure 4.1. Engagement and disengagement of the tether is completely passive. The rear membrane pulls the tether when there is no vacuum in the plenum. When a partial vacuum is induced in the plenum, the rear membrane deflects under the pressure load and releases the tether.

The tether hardware is shown in Figure 4.2. Two plastic disks sandwich the front membrane. The point of contact with the membrane is radiused to minimize local bending stresses in the membrane. A threaded rod is fastened to the disks and passes through a plastic access plate on the rear membrane. A double nut serves as an adjustable stop. The access plate is threaded into a mating flange that is fastened to the rear membrane. Two 0.10-mm (4-mil) stainless steel doublers are used to distribute loads through the membrane.

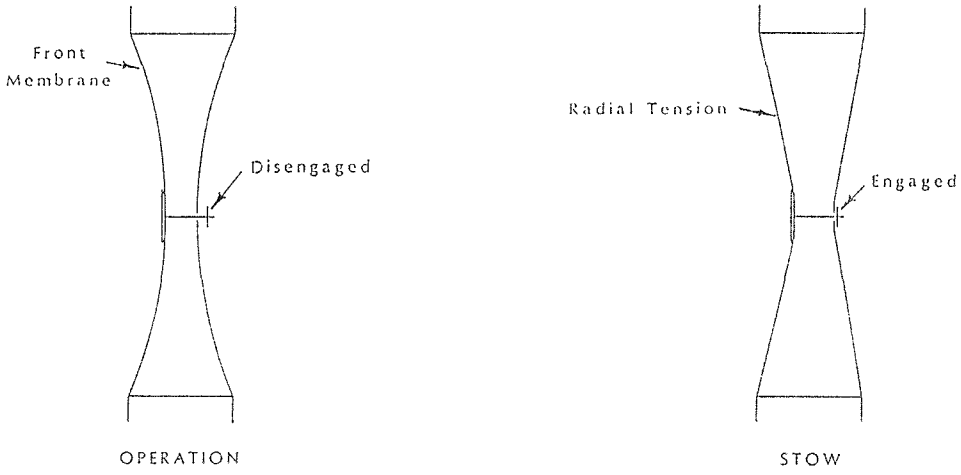

Figure 4.1 Passive Tether Operation.

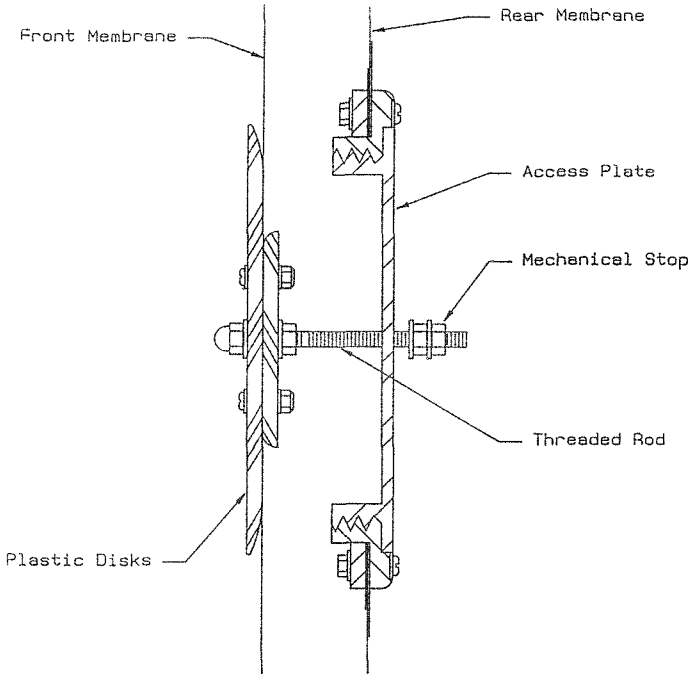

Figure 4.2 Tether Detail.

4.4 REAR MEMBRANE

The rear membrane is designed to close the plenum and to engage and disengage the tether. This membrane is initially flat. It is not plastically formed so that it will have sufficient elastic spring-back to pull the tether to the rear when the operational pressure is removed. It was originally specified as 0.08-mm (3-mils) thick, but tests showed the onset of yielding. The thickness was subsequently increased to 0.10 mm (4 mils).

In the initial test, a 0.08-mm (3-mil) membrane was installed on the 3.7-m diameter tooling ring. The center deflection from the weight of the membrane was recorded. The load was incrementally increased to the operational level, and the center deflection was measured after each increase. Figure 4.3 shows the gradual increase in center deflection. The theoretical stress in this membrane was well below the measured value of 310 MPa (45,000 psi), and there is no knee in the curve indicating the onset of gross yielding. The interpretation of this data is that the membrane was yielding locally. The membrane was not perfectly flat initially. There were slack areas from coil stock and seam welding inconsistencies. Therefore, the stress could be very nonuniform and local yielding could occur. If the facet membrane yielded significantly, it would not be capable of engaging the tether. Therefore, a 0.10-mm (4-mil) rear membrane was selected to avoid this uncertainty. The 0.10-mm (4-mil) membrane used on the facet worked well. No yielding was measured, and it readily engaged the tether.

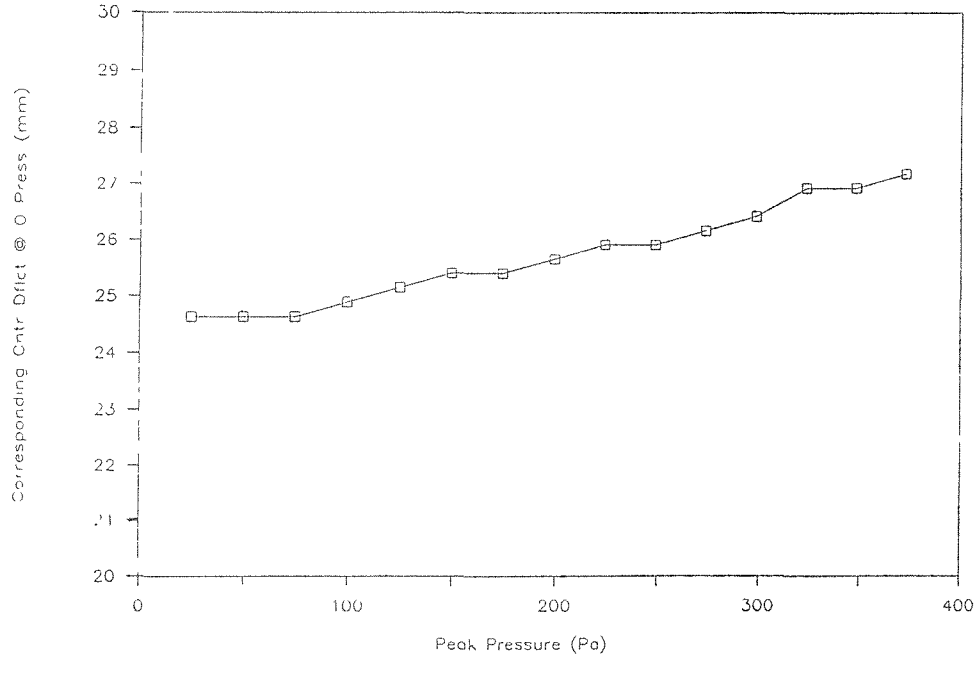

Figure 4.3 Change in Center Deflection During a Test of a 0.08 mm (3-mil) Rear Membrane.

The rear membrane is installed on the ring with initial tension to ensure good spring-back. The minimum required tension was estimated to be 2100 N/m (12 lbs/in). Since the membrane and ring have different coefficients of thermal expansion (CTE), the level of tension changes with temperature. The tension decreases with increases in temperature. Therefore, the membrane was tensioned so that it would have 2100 N/m (12 lbs/in) at the highest required survival temperature of 50 °C (122 °F).

The tension created by a temperature drop is dramatic. The initial tension is 13,000 N/m (73 lbs/in) at the lowest operational and survival temperature of -30 °C (-22 °F). For room temperature assembly, the initial tension should be approximately 5300 N/m (30 lbs/in). These calculations are based on the assumption that the ring will compress from the increased tension but will not roll. Any roll would reduce the membrane tension. This seems to be a reasonable assumption when one considers that the tension in the front membrane caused by the operational pressure will reduce the roll moment.

An annealed 0.10-mm (4-mil) rear membrane may be stressed to yield if a combination of worst conditions exists. If the temperature is -30 °C (-22 °F), the operational pressure is on, the wind gusts to 22 m/s (50 mph), and the rear membrane is facing directly into the wind; then, the stress level would reach 240 MPa (35,000 psi), which is the minimum yield strength for annealed 304 stainless steel.

Slight yielding of this membrane is not necessarily bad. Yielding would be self-limiting (due to geometry of the loading and the high plastic modulus) and would not result in rupture. Slight yielding would be tantamount to a reduction in the initial tension. More yielding could make the tether ineffective at high temperatures, which would put the front membrane in danger.

Changes in the design were made to prevent yielding even though the conditions that impose these loads are a very unlikely combination of worst cases. SKI felt that it was more prudent to use a work hardened material than risk facet failure. Quarter hard, 0.10-mm (4-mil), 304 stainless steel was selected for the rear membrane. The minimum yield strength is 520 MPa (75,000 psi), and the percent elongation is 31%. The disadvantage of using a hardened alloy is the complexities associated with ensuring that the weld heat does not adversely affect the local properties. There is a slight cost penalty at low-volume production because of the material availability, but it is expected to be insignificant or even a cost advantage at high production rates.

5.0 RING DESIGN

The design of the ring was a critical step in the facet design because the ring represents the majority of the facet weight. The ring was designed to survive worst case loads without structural failure. The resulting ring was sufficiently stiff to avoid excessive optical distortions during operation. This section of text describes the key assumptions of the ring design, describes the loads used in the analysis, summarizes the analysis, and presents the results.

The ring was originally sized assuming a 0.08-mm (3-mil) rear membrane. The rear membrane was later changed to 0.10 mm (4 mils), and the analysis was repeated to ensure the adequacy of the ring design. The change in rear membrane thickness caused some factors of safety to shrink, but remain within acceptable limits.

5.1 KEY ASSUMPTIONS

The key assumptions of this analysis are listed below. The logic behind most of these assumptions is provided later in this section.

1. 0.10-mm (4-mil) rear membrane.
2. Wind speeds (including gusts):
   a. 12 m/s (27 mph) during operation,
   b. 22 m/s (50 mph) any orientation, and
   c. 40 m/s (90 mph) in stow.
3. Stow orientation with dish facing zenith.
4. Uniform pressure profile on facet for all cases.
5. Wind force coefficients same as heliostat.
6. f/D range of 2.72 to 3.0.
7. Operational pressure of shortest focal length used with 12 m/s and 22 m/s cases.
8. Initial tension of 2100 N/m (12 lbs/in) @ 50 °C (122 °F).
9. Temp of -30 °C (-22 °F).
10. Prototype diameter of 3.58 m (140.9 inches) reflective aperture.
11. Point radial loads insignificant.
12. Ring structurally coupled to membranes.

The prototype and commercial facets differ in radius by a few inches. Sandia and SKI decided to change the diameter of the commercial unit so that it could be shipped without exceeding highway height and width standards. This change was made after most of the ring design work was completed. The commercial ring outside diameter will be no larger than 3.60 m (141.7 inches). The prototype ring outside diameter is 3.67 m (144.5 inches). The design, analysis, and costing are based on the prototype size. The small difference is not expected to make a large impact on either the weight per unit area or cost of the facet.

5.2 LOADS

For this analysis, ring loads considered were wind, operational pressure (plenum vacuum), initial membrane tension, and membrane load from change in temperature. Five cases were considered: one operational, two 22 m/s (50 mph) survival, and two 40-m/s (90-mph) survival.

Wind loads were based on wind tunnel tests of heliostats and dishes performed by Colorado State University. Test results for heliostats were assumed to be most representative of any given facet, but existing heliostat data is inaccurate due to minor testing errors (Ref. 8). This inaccuracy was avoided by using reliable dish drag coefficients for head-on cases (Ref. 8). This was justified because earlier tests showed that the drag coefficients for dishes and heliostats are within 10% of each other for the head-on case (Ref. 9). Load reductions for other orientations were then based on the relative load reduction tested in heliostats (Ref. 10). The resulting normal load coefficient for the head-on cases (12 m/s and 22 m/s) was 1.6 and for the stow cases was 0.8. Mean load coefficients were used with the given peak wind speeds. The facet angle of attack (angle between facet ring plane and wind vector) for a dish in stow was based on the outer most facets. This angle was 0.35 radians (20 degrees).

For each case, it was assumed that the wind load resulted from a gust rather than a steady wind. Because of this, it was assumed that the pressure profile does not have enough time to develop on the leeward face of the facet, and the entire wind load is carried by the windward membrane. This is conservative because it results in the highest differential tension between the front and rear membranes. This differential tension induces ring roll.

The operational pressure varies between the facets of the dish depending on the facet focal length. For analysis, it was conservatively assumed that the operational pressure was the highest of all the facets. This was calculated to be 1000 Pa (0.15 psi).

We also assumed that the load from the operational pressure and the wind would occur simultaneously during operation. It was assumed that they could occur simultaneously for the 22 m/s (50 mph) cases because of the low leak rate for the facet. The 22 m/s (50 mph) cases are of interest because they represent the scenario where an operating dish has received a go-to-stow signal but has not reached stow prior to the wind increasing to 22 m/s (50 mph). Although the fan inducing the operational pressure would have stopped, it is likely that a large portion of the vacuum pressure would remain.

Table 5.1 summarizes the resulting radial ring loads for each of these cases. Note that the highest total membrane load (front and rear) occurs with a 22 m/s (50 mph wind), and the highest induced moment (caused by the difference of the two) occurs with a 40 m/s (90 mph) rear wind.

Table 5.1
Ring Loading

Case #	Wind Speed (mph)	Wind Speed (m/s)	Wind Direct.	Angle of Attack (degrees)	Op. Press (psi)	Op. Press (Pa)	Mem. Tension (lbs/in) Front	Mem. Tension (lbs/in) Rear
1	27	12	Rear	90	0.15	1000	57	124
2	50	22	Front	90	0.15	1000	84	118
3	50	22	Rear	90	0.15	1000	57	141
4	90	40	Front	20	0	0	46	73
5	90	40	Rear	20	0	0	0	107

Gravity and wind loads acting normal to the ring plane have been included in the analysis, but gravity and wind loads acting in the plane of the ring have been neglected. It was assumed that there would be only a small effect on the ring from the three supports carrying the weight of a facet facing the horizon. This assumption was based on the relative magnitude of weight and membrane tension and on the likely effectiveness of membranes in distributing this load. The facet weight is 119 kg (261 lbs) and is carried by three brackets with 25 cm (10 inch) wide feet compared to a maximum radial load from the membranes of 35,000 N/m (200 lbs/in).

5.3 ANALYSIS

Carbon steel was selected for the ring material due to its low cost and relative compatibility with the stainless steel membranes (closer CTE match than aluminum). A low carbon, commercial quality steel was selected as opposed to a high strength steel because the higher strength was not needed. The limiting criteria for the ring was stability, not strength. ASTM A 570-grade 30 was selected because of its low cost.

Heliostats are structurally efficient and lightweight because the membranes add stiffness to the ring. For any ring to deflect out-of-plane, it must roll (the top surface will roll outward at midspan and inward at the supports for a downward deflection). The membranes are very stiff in the radial direction and resist this radial motion. By resisting the radial motion, the membranes restrict ring deflection. It was assumed that the facet would have coupling between the membranes and ring similar to a heliostat. This was an assumption because the membranes have deeper contours than heliostats and are less resistant to radial motion. This very important assumption is not conservative, but is supported to some extent by subsequent hardware tests. Radial deflection of the facet ring under the weight of the facet was measured and found to be unobservably small (less than 1 mm (0.04 inches)). If the membranes had zero radial stiffness, the deflection would have exceeded 3 mm (0.12 inches). This supports the coupling assumption because, in spite of the membrane contour, the membranes have high radial stiffness.

A ring height of 20 cm (8 inches) was selected based on geometric clearance requirements for the membranes. The front membrane has a deflection of 8.4 cm (3.3 inches),

and the rear membrane could have a deflection of 5.6 cm (2.2 inches). The remaining 6.3 cm (2.5 inches) is space for the tether and some nominal clearance. The tether was later designed to take up only about one inch. Therefore, it would be possible to slightly reduce the ring height and weight beyond the current design.

A channel was selected as the ring shape because it provides a landing and edge for attachment of the membranes and because it only has one web. The same amount of material used in a rectangular tube would have much thinner webs and would suffer web buckling at much lower loads and would be more difficult to roll. A two-inch flange width was arbitrarily selected to be sufficient for membrane attachment and to provide some in-plane moment of inertia.

The remaining task of the ring analysis was to define a ring material thickness that would not structurally fail or deflect excessively under operational loads. Ring height and flange width can be set to any value desired because the ring is made from sheet stock. The thickness, however, is limited to commercial gages and can only be varied in established increments.

A two-term design approximation (Ref. 11) technique was used to analyze the coupled structure of the facet and ring. The analysis also included the effects of ring roll from the distributed moment but neglected the discreet moments from the three supports. It was assumed that the ring was simply supported. Also included in the analysis were the effects of the ring cross section distorting or bowing due to the membrane loads on top and bottom. The stress from cross-section distortion and ring bending between supports is small. For case number 3, the worst case, cross-section distortion and ring bending each represented only 5% of the total ring stress. The stress due to the distributed moment was 40% of the total, and the stress due to axial compression was 50% of the total. Peak principal stress was 131 MPa (19,000 psi). Peak operational principal stress (case 1) was 110 MPa (16,000 psi).

5.4 RING FAILURE MODES

The following six failure modes were considered: material yield, web buckling, flange buckling, radial ring buckling, out-of-plane ring buckling, and optical distortion due to ring deflection. The factor of safety for each failure mode was calculated for each of the design cases and was judged to be adequate. Factor of safety is defined as the ratio of actual stress to the theoretical stress limit. Peak principal stresses are used for yield analysis. True peak stresses are used for buckling analysis.

For yield, the theoretical limit was the published minimum yield strength of the material 207 MPa (30,000 psi). Theoretical limits for web and flange buckling were defined using classical techniques presented by Timoshenko (Ref. 12). The method for determining the radial and out-of-plane buckling limits for the coupled structure are defined by Murphy (Ref. 13). The effect of ring sag on the optics was predicted using a method presented by Murphy (Ref. 11) for stretched-membrane heliostats. The effect of radial deflections on membrane optics was neglected because of the shallow

membrane-to-ring-plane departure angle. Ring roll induced unloading of the membrane is expected to be insignificant because of the low ring sag. Peak operational ring sag is expected to be 0.15 mm (0.006 inches).

The material selected for the ring is based on this analysis is 11 gage (3.0 mm (0.12 inches thick)). The factor of safety for each failure mode is shown in Table 5.2. These values are for case 3, which is the most severe of the cases in terms of stress.

Table 5.2
Factor of Safety

Yield	1.6
Web Buckling	2.3
Flange Buckling	2.3
Radial Ring Buckling	43
Out-of-plane Buckling	17

Theoretical limits for buckling are seldom reached with actual hardware because of initial imperfections. Failure at 50% of yield is not uncommon (Ref. 14). For this reason, factors of safety on buckling are generally larger than what is typically used for yield. A factor of safety of 2.3 on buckling was judged to be low, but acceptable.

Web buckling was judged to be the limiting factor in this design. Flange buckling limits could be easily improved by small reductions in the flange width. The factor of safety on yield is sufficient; but if it were limiting the design, materials with higher yield strengths could be used with only slightly higher costs.

The loads are reached under a rather severe combination of circumstances. We have assumed the combined effect of severe cold (-30 °C, -22 °F), high wind (22 m/s, 50 mph), and worst orientation (head-on) combined with operational pressure in the facet. These worst-worst conditions are highly unlikely, and make the likelihood of failure remote, and the low safety factor on wall buckling acceptable.

Snow and ice loads were not combined with these other loads. Snow and ice loads of 50 kg/m^2, as defined by the statement of work (Ref. 15), impose the same pressure on the facet as a 22 m/s (50 mph) wind with the drag coefficients used here. Snow and ice is not a limiting load since it would not be compounded by the vacuum load, and it would be acting on the front membrane (which carries loads more efficiently because of its contour).

5.5 RESULTS

The ring was designed using low-cost carbon steel in sheet form. The sheets are formed into a channel and rolled into a ring with legs facing radially outward. The ring is 20 cm

(8 inches) high with 5 cm (2 inch) flanges and is 3 mm (0.12 inches) thick. The weight of the ring is 83 kg (182 lbs), which is 8.3 kg/m^2 (1.7 lbs/ft^2) of aperture area. The ring is painted for rust protection.

Table 5.3 summarizes the weight of the facet. All items that are contained within the facet envelope are included here. Focus control components are not. With the next design iteration, it may be possible to reduce the ring height (and weight) based on the clearance between the two membranes.

Table 5.3
Facet Weight Summary

	kg	lbs
Ring with doublers	82.7	182
Front Membrane (with ECP)	7.3	16
Rear Membrane	8.6	19
Clips	9.1	20
Support Assemblies	10.0	22
Tether	0.9	2
Total Facet Weight	118.6	261
Total Facet Weight	11.7 kg/m^2	2.4 lbs/ft^2

6.0 MEMBRANE-TO-RING ATTACHMENT

Attachment of tensioned stainless steel membranes to a carbon steel ring presents an interesting design challenge. SAIC has welded stainless steel membranes to a carbon steel ring electroplated with nickel (Ref. 16) for similar applications. Recently, SAIC constructed a prototype heliostat using stainless-to-carbon steel welds without nickel plating (Ref. 17). The classical problem with such welds is corrosion induced by the differing galvanic potential of the metals. The nickel plating was intended to prevent this and has survived well since July 1988. Longevity of nickeless welds have yet to be demonstrated. SKI decided to mechanically (with fasteners) attach the membranes to the ring. This decision was made to avoid the uncertainty of nickeless welds and to not incur the development effort and uncertainty associated with electroplated welds (note that this decision was made when SAIC's electroplated module was less than 14 months old).

The concept selected by SKI uses a clip to clamp the membrane against the ring as shown in Figure 6.1. The membrane is held in place by a combination of the friction under the clip and the resistance provided by wrapping the membrane around the edge of the flange. The requirements for the clip were that it allow no slippage of the membrane under survival conditions. This was analytically determined to be 24,700 N/m (141 lbs/in) for the rear membrane and 15,000 N/m (84 lbs/in) for the front. The worst case loading occurred with a gust to 22 m/s (50 mph) on a cold facet facing the horizon away from the wind.

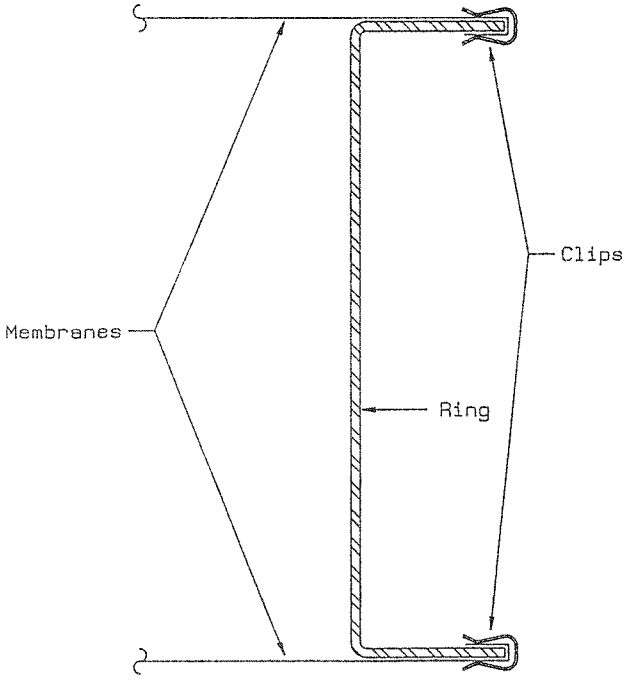

Figure 6.1 Geometry of Clip, Ring, and Membranes.

The material selected for the clip was 301 half-hard stainless. The material was selected for its high strength, corrosion resistance, and sufficient ductility to allow the clip to be formed from sheet stock. The clip would be manufactured in a continuous strip equal in length to the outside circumference of the ring flange and slotted to allow it to bend to the contour of the ring (See Figure 6.2).

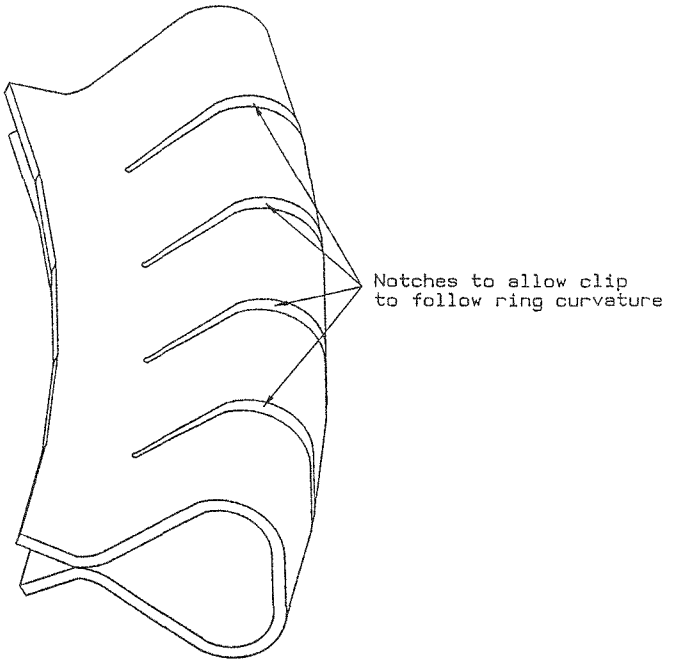

Figure 6.2 Commercial Clip.

The baseline clip was designed, and tests were done to define material thickness. The first prototypes were formed from 22 gauge (0.7 mm (0.029 inches) thick) as shown in Figure 6.3. Four-inch long clips were made and tested with one-inch wide membrane material. The membrane material used for testing was actual membrane material taken from trimmed scrap (0.08 mm (3 mil) thick with ECP laminated to it for the front membrane and 0.10 mm (4 mil) for the rear membrane). A strip of front membrane material was folded around a section of ring flange, and a test clip was pressed onto the flange over the test strip. A 45 kg (100 pound weight) was hung from the test strip. After an initial 0.8 mm (0.03 inches) of slip as the load was applied, the clip held the weight without slippage for three days. After three days, 14 kg (30 pounds) was added. Once again, an initial 0.8 mm (0.03 inches) of slip was noticed as the weight was added after which the weight was left for two days with no further slippage. The weight was then increased to 66 kg (145 pounds), and the strip pulled completely out of the clip four hours later.

The next test was with a piece of rear membrane (0.10 mm (4 mil) thick). A 45 kg (100 pound) weight caused an initial slippage of about 0.18 mm (.007 inches), and then,

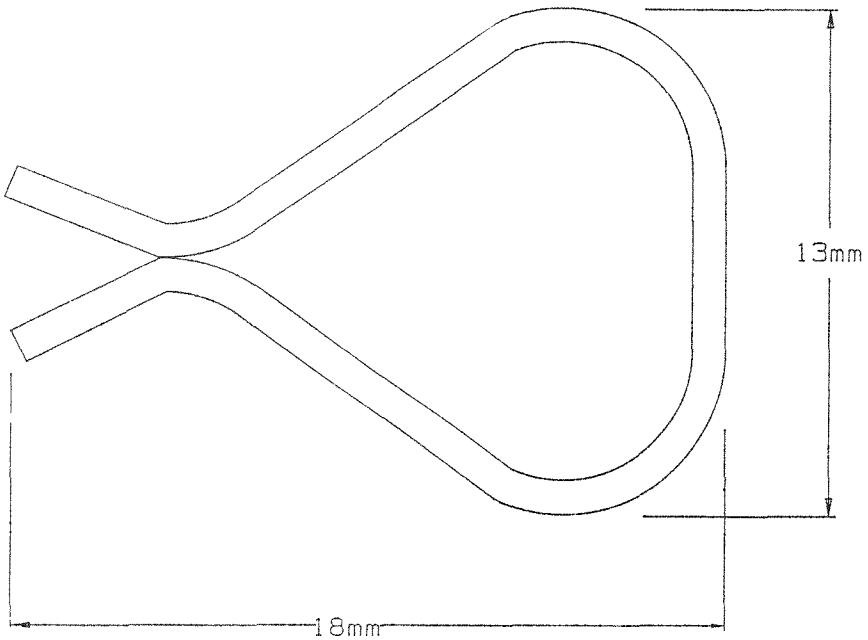

Figure 6.3 Clip Size.

it held overnight. Adding another 14 kg (30 pounds) to the weight caused the strip to pull out immediately. Due to the initial slippage we experienced and the rear membrane failure at only 59 kg (130 pounds), the decision was made to increase the clip material to 20 gauge (0.91 mm (.036 inch) thick), thereby, increasing the clips stiffness and clamping force.

The first testing with the new clip was with 0.10 mm (4-mil) thick rear membrane. Hanging 45 kg (100 pounds) of mass caused no initial slippage. After one day, another 14 kg (30 pounds) was added causing initial slippage of 0.8 mm (0.03 inches). The 130 load was left hanging for two days; then, another 14 kg (30 pounds) was added for a 73 kg (160 pound) total. The initial slippage was over 25 mm (one inch).

It was decided that a rougher surface finish on the ring flange increasing the coefficient of friction would eliminate the initial slippage problem. The flange surface was sandblasted with a medium grit blast material.

We hung 82 kg (180 pounds) on a 0.10 mm thick, 25 mm (one inch) wide strip of stainless steel. No slippage was observed. We hung 59 kg (130 pounds) on a 25 mm (one inch) wide strip of laminated 0.07 mm (3 mil) thick front membrane materials. No slippage was observed after several days.

Corrosion of the carbon steel in the joint area can be prevented by application of a sealant. A low viscosity sealant would be required to penetrate all areas.

7.0 FACET SUPPORT DESIGN

The hardware used to support the facet was designed to meet the following objectives:

a. Provide three points of support for the facet,
b. Allow for fabrication tolerances of dish structure and facet,
c. Provide means for facet alignment,
d. Avoid inducing excessive stresses or deflections in ring,
e. Allow for in-plane dish structure motion, and
f. Be durable and inexpensive.

Figure 7.1 shows the hardware that met these objectives. A steel weldment attaches to the ring with six bolts. A threaded rod passes through holes in the bracket and the dish. A urethane washer set is used at the top, and two spherical washer sets are used at the bottom of the threaded rod.

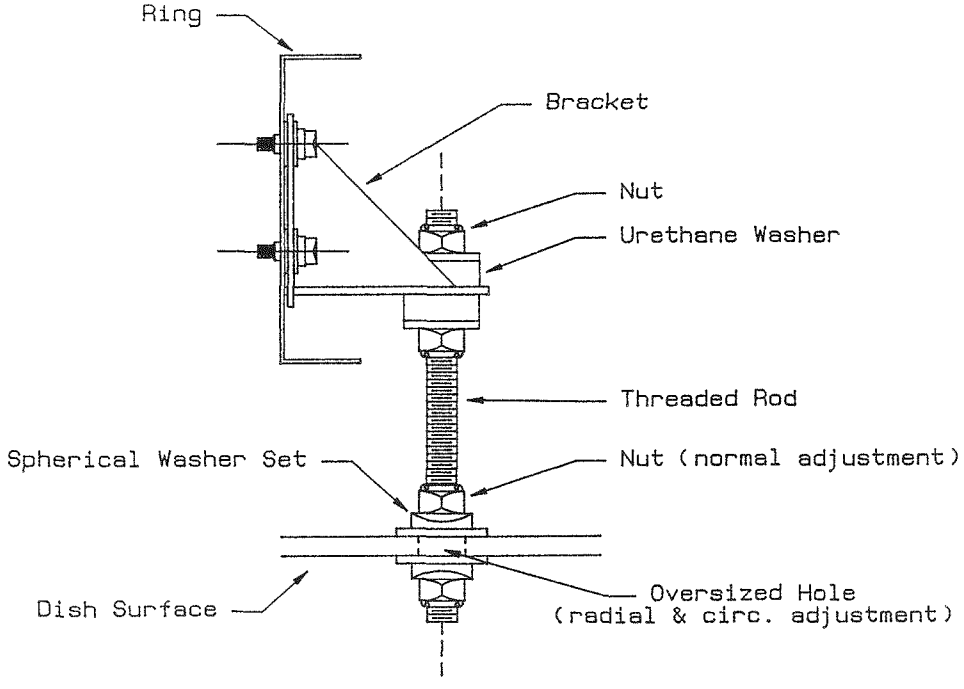

Figure 7.1 Facet Support Hardware.

Fabrication tolerances of the dish structure and the facet are allowed by an oversized hole in the facet support structure of the dish. The hole is currently planned to be 13 mm (0.5 inches) oversized. This would accommodate a total of +/- 6 mm (+/- 0.25 inch) tolerance for both the dish and facet. Two plate washers are used to span the

oversized hole. Rotational tolerance of the dish and facet are allowed by the two spherical washer sets. The rotational freedom of the washer sets will be eliminated by tack welding the mating parts of the washers together after installation and alignment. This joint will act as the fixed connection.

Facet alignment can be accomplished by adjusting the lower two nuts. The thread pitch is 16 threads per inch. This will allow fine adjustment (0.1 mrad per quarter turn of the nut).

The loads are carried into the ring through the brackets. The brackets are ten inches wide, and each is mounted to the ring with six bolts to avoid concentrated ring loading. The rod is kept as close as practical to the shear center of the ring to limit the magnitude of discreet moment loads. In the structural analysis of the ring, we assumed simple supports at these locations. Adequacy of these details was based on engineering judgement.

Ideally, the three mounting points on the dish would not move relative to one another after the facet was installed. In practice, the three points have relative motion due to the structural response of the dish from variable wind and gravity loads. If the facet was not adequately isolated from this motion, unacceptable ring distortion or stresses could result. The support design provides this isolation with a thin rod and a soft upper attachment. Figure 7.2 qualitatively describes these considerations. An overly stiff rod is shown on the left. Ring translation would directly follow dish translation. A thin rod with a hard upper attachment is shown in the center. Translation of the dish would not cause ring translation (due to structural resistance of the ring), but would result in ring rotation. The figure on the right shows the isolation provided by a thin rod and a soft upper attachment.

The analysis of this support was performed prior to the design of the dish structure and was, therefore, based on budgets for dish deflections. A budget of 3 mm (0.12 inches) of relative motion 1.5 mm (0.06 inch each) was selected based on discussions with WGAssociates. Allowable ring load from this source was set to that which would be caused by gravity when the dish faced the horizon. This limit was selected without the detailed analysis that would be required to define the true allowable limit. A 19-mm (0.75-inch) threaded rod satisfied this criteria. It would allow 1.5 mm (0.06 inches) of translation without inducing excessive force on the ring. The bending stress in the rod would be limited to 340 MPa (50,000 psi). Grade 5 provided an adequate safety margin on yield (1.6). Compliant urethane washers were specified for the attachment of the rod to the bracket so that no rotation would be induced into the bracket from the rod. Approximately 18 mrad of rotation of the end of the rod is expected when the rod is bent. The compliant washer isolates the bracket from this rotation. The washers are not so compliant that they would fail to maintain facet alignment. Operational compression of the washers will result in only 0.08 mm (0.003 inches) of deflection.

Urethane washers were selected over machined bearings based on cost-effectiveness. Urethane is weatherable and durable. The bracket is equally cost-effective. It is a weldment of four sheared and punched parts.

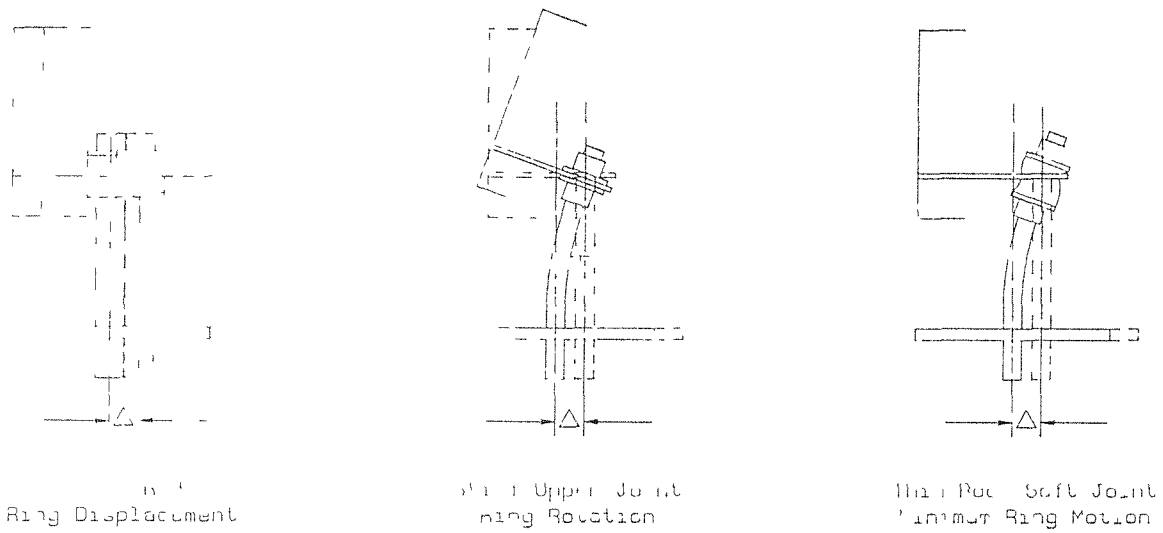

Figure 7.2 Conceptual Effects of Some Support Hardware Variables.

8.0 FOCUS CONTROL SYSTEM DESIGN

The focal length of each facet is held constant by maintaining a predetermined differential pressure across the front membrane. The system that generates and controls this pressure differential is the subject of this section of the report. Concept selection is presented first, followed by a description of the system and discussions of optical performance and parasitics.

The concept that was initially proposed for focus control maintained constant membrane position (rather than pressure) with a valve whose orifice was attenuated by the front membrane when it reached the proper position. This concept was not adopted because of the need for a steady reference location for the valve. If the valve was located near the facet center, a deflection of the valve of 1.3 mm (0.05 inches) with respect to the ring plane would cause a slope error of approximately one mrad. Three options were considered for placement and referencing of the valve: the rear membrane, a cantilever arm attached to the ring, and the center of a beam spanning the ring diameter. The rear membrane was desirable because it added little additional hardware. However, the rear membrane's position varied excessively with changes in wind pressure. The cantilever arm was rejected because of potentially excessive ring roll. Ring roll would translate the valve and change the facet focal length. The magnitude of ring roll is dependent on membrane/ring coupling and was not defined. An independent diametral beam of sufficient stiffness would weigh approximately 5 kg (11 pounds) (aluminum at $1.60 per pound). This approach was undesirable because of the associated cost and complexities.

Focus control based on sensing and maintaining a differential pressure was pursued as an alternative. A passive diaphragm-type vacuum regulator was investigated as a means of pressure control. These regulators use the pressure differential (pressure acting on the front membrane) to operate a valve via a diaphragm. The natural gas industry uses such regulators and their use in such applications has proven to be reliable. The operating conditions for focus control were not typical for the industry. Typically, there is a large difference in pressure between the regulator inlet and outlet. The low pressure difference in our application reduced the repeatability of the regulator. Tests were conducted with a regulator using the first facet. These tests showed an unacceptable repeatability for that particular regulator. Other regulators that were better suited for this application (larger diaphragms and valves) were not readily available from the manufacturer and could not be tested. Although passive regulators have the desirable traits of simplicity, reliability, and zero parasitics, the possibility of their use could not be established.

The selected approach to pressure control is a solenoid valve activated by a pressure switch. The solenoid valve is opened and closed by two contacts in a pressure switch. Although these components are not passive, they are common industrial equipment with a long history of proven reliability.

One side of the pressure switch is plumbed to the facet plenum, and the other side to the front face of the facet. The accuracy of the reading is increased by including the effects of dynamic pressure as opposed to referencing only to the static pressure. The dynamic pressure from a 7.6 m/s (17 mph wind) (the mean wind associated with gusts to 12 m/s (27 mph)) could cause the focal length of the facet to change by 15 cm (6 inches), and induce one mrad of error. A small weather shield is placed over the tap to prevent water and dirt intrusion. This shield does not alter the pressure reading.

The facets are positioned on the dish such that several facets have identical focal lengths. This allows ganging of these facets with one controller (one valve/switch combination per gang). Figure 8.1 is a flow diagram for the entire system showing the ganging. Each gang has a valve/switch combination and an over pressure switch to stop the blower if the plenum vacuum becomes excessive. The facet vacuum will exceed its limit if the temperature of the gas in the facet decreases rapidly. Large, rapid changes in temperature are not expected to occur during dish operation. One blower supplies the vacuum source for all gangs.

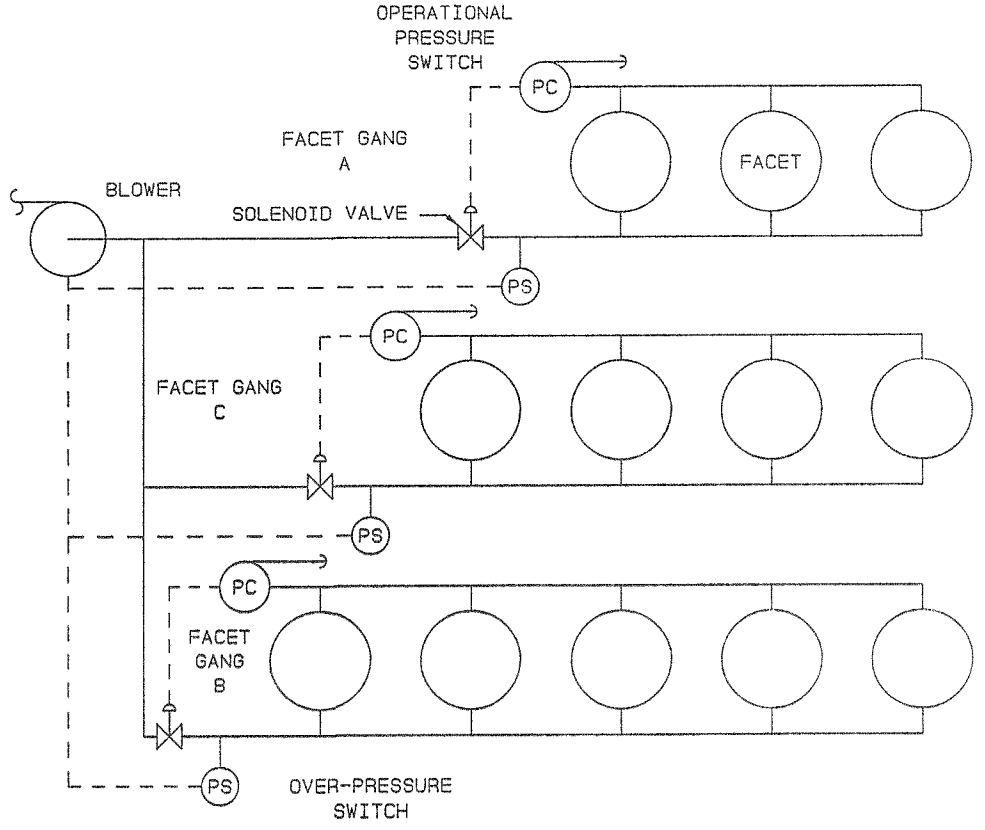

Figure 8.1 Flow Diagram of Focus Control System.

One facet in gang A and one facet in gang B has a slightly different focal length than the others in the gang. The dish performance impact of this is expected to be small. Table 8.1 shows the ganging and ideal focal lengths of each facet. Figure 8.2 shows the facet numbering pattern used for this table. The imperfect focal length of the two facets

affects performance in that their flux pattern is spread at the receiver plane. The impact can be judged in terms of an equivalent RMS slope error that causes a similar spread. As is shown in Table 8.1, the resulting error is 0.7 mrad for one facet and 1.3 mrad for the other. This is roughly equivalent to the error of each of the twelve facets being increased by 0.23 mrad. Without doing a more thorough analysis to predict actual dish performance, this penalty was judged to be acceptable.

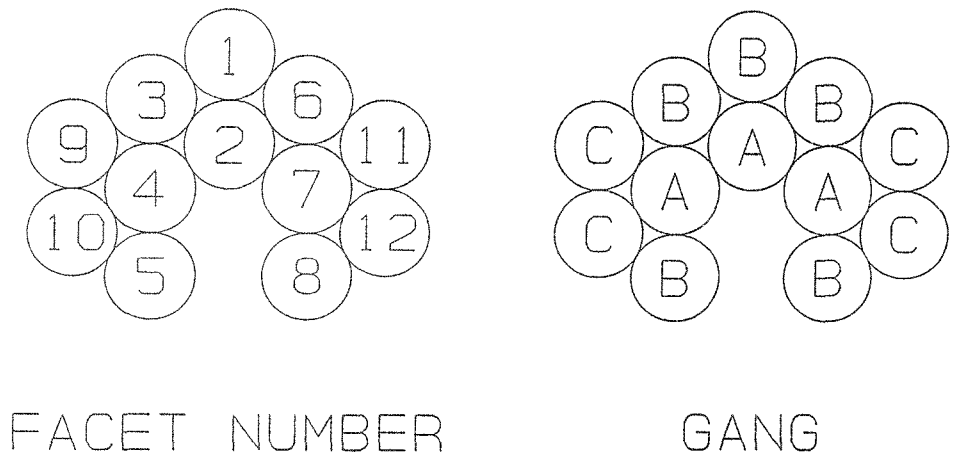

Figure 8.2 Facet Number and Gang Identification.

A potential problem of this ganging scenario is the hot spots created in the receiver as a result of the two facets with imperfect focal lengths. Acceptable limitations for this were reviewed early in this project without success.

With further receiver development and testing, a realistic limitation may be found. Two options are available if the two facets are not within these limits. First, the distance from the receiver to the facet may be increased by a combination of facet mount adjustment, facet support bracket modification, and dish hardware modification. Secondly, two new gangs could be added for control of these two facets.

Table 8.1
Facet Ganging for Purpose of Focal Length Control

Facet #	Ideal f(m)	Gang	Actual f(m)	Resulting Slope Error (mrad)	Total Slope Error (mrad)
2	9.5	A	9.6	0.7	1.8
4	9.6	A	9.6	0	1.1
7	9.6	A	9.6	0	1.1
8	10.0	B	10.0	0	1.1
3	10.0	B	10.0	0	1.1
5	10.0	B	10.0	0	1.1
6	10.0	B	10.0	0	1.1
1	10.2	B	10.0	1.3	2.4
9	10.5	C	10.5	0	1.1
10	10.5	C	10.5	0	1.1
11	10.5	C	10.5	0	1.1
12	10.5	C	10.5	0	1.1

RMS = 1.33 mrad
Net Increase = 0.23 mrad

The parasitic power requirements of this control system were estimated based on product specifications and experience with the prototype. The power consumption of the second prototype facet was measured to be 42 watts with the blower operating 30% of the time for an average power consumption of 13 watts. The flow rate was not measured, and therefore, an accurate estimate of the parasitics for one blower and 12 facets could not be made. This was further complicated by the differences between the prototype and commercial blower. Following discussions with factory engineers, an estimate of 100 watts was selected with the blower running continuously. Solenoid specifications for the solenoid valves state they consume 16 watts when open. If they are open 30% of the time, the three valves would consume an average of 14 watts. Similar estimates for relays and miscellaneous equipment suggests 140 watts of parasitic power are required for the entire system. The uncertainty of this estimate is large, but there is confidence that the parasitics will be below 1% (250 watts) of the dish output of 25 kW_e.

9.0 COMMERCIAL COST-STUDY

The cost to manufacture stretched-membrane facets on a commercial scale was evaluated. This effort was intended to provide cost projections so that the economic merit of the faceted-membrane concept could better be evaluated. It was also intended to provide a basis from which comparisons could be made with developers of other membrane facets. This work was limited to the current facet design and included the facet focus control system. Material requirements were based on the size of the prototype unit. Commercial units may have slightly different diameters, but cost per unit aperture is assumed to be representative. The following three production rates were considered: 500, 1000, and 10,000 facets per year. Vendor quotes were used for most of the direct material costs. Engineering judgement was used to estimate the manufacturing requirements. The business related expenses were based on SKI's experience as a small manufacturer. Shipping and installation costs have been provided to WGAssociates and have not been included here.

SKI worked with SAIC on many of the assumptions for this analysis. Commonality of assumptions was desired in order to make a valid comparison of the costs of the two facet designs. Several key assumptions are common to the two contractors' studies and are identified in this section. Many assumptions were made that are not consistent with SAIC. These were made of necessity because of the different cost accounting methods used by the two companies and the different materials used in the facets. We believe that our costs are appropriate for our company's capabilities and costing structure.

The direct material costs (costs of the raw material and purchased parts) strongly influence the facet costs. These costs were based primarily on vendor quotes. Engineering judgement was applied on many of the minor items and on those items for which quotes were difficult to obtain. The cost of the reflective film was set at $\$21.53/m^2$ ($\$2.00/ft^2$). The facet cost is very sensitive to this single value because it represents over 50% of the direct material cost. Arguments can be made for lower film costs based on anticipated competitive film market, but $\$ 2.00/ft^2$ is the price 3M currently quotes for film purchased in large volume. This is the value used for this cost study and is the value used by SAIC. The cost for paint is also consistent with SAIC. Other material costs differ from SAIC's because of different materials (tempers, alloys, forms) and components.

Table 9.1 summarizes the direct material costs for our facet. A complete breakdown of these costs is provided in appendix A.

Table 9.1
Direct Material Cost Summary ($/facet)

	Annual Production Rate		
	500	1000	10000
Film	214.0	214.0	214.0
Membranes	43.2	41.6	40.6
Ring	47.1	44.9	43.3
Clips	27.5	27.5	27.0
Controls	43.9	43.8	32.9
Other	47.0	46.6	45.8
Total	422.7	418.4	403.6

Estimates for tooling and labor are based on SKI's experience with the production of parabolic troughs and light fixtures. The equipment and labor required to manufacture the major components were identified. No unusual production processes are required to fabricate the stretched-membrane facets. The ring, membranes, and the clips are all made from coil stock (in sheet form). The ring is first made into straight channels using a roll former. It is then "bent" to the desired radius with a set of pyramid rolls. The membranes are seamed together with electric resistance seam welders with the front membrane material first laminated in a dry pinch roll process. The clip material is first slit to width, punched, and then rolled to the proper profile. Assembly of the facet is done in a fixture that provides accurate placement of the parts. Ring and facet transfer is facilitated by a series of lightweight, overhead, manual trollies. The cost for the equipment has been estimated. Table 9.2 provides a summary of the labor and tooling costs. A more detailed summary is provided in appendix B.

Table 9.2
Labor and Tooling Cost Summary

	Annual Production Rate		
	500	1000	10000
Labor Hours	13.6	13.6	5.2
Tooling Costs ($M)	0.63	0.63	1.33

The manufacturing process for production rates of 500 and 1000 facets per year are very similar. Production scenarios and efficiency would be expected to change slightly, but are not significant in terms of the uncertainty of the current estimates. For this reason, it was assumed that the same equipment could be used for either production rate and that the man-hours per unit would be the same. Note that at a production rate of 10,000 units per year, more automated (and costly) equipment would allow for fewer man-hours per part.

The business related expenses are based on assumptions typical of a small business. These assumptions are summarized in Table 9.3 and defined as follows:

Table 9.3
Business Related Assumptions

	Annual Production Rate		
	500	1000	10000
Material Overhead (%)	10	10	5
Direct Labor Rate ($/Hr.)	9.00	9.00	9.00
Labor Burden (%)	70	70	50
R & D (%)	3	3	3
G & A (%)	35	25	15
Cap. Depreciation Schedule (Yrs.)	7	7	7
Federal Income Tax (%)	34	34	34
State Income Tax (%)	4	4	4
Inflation Rate (%)	4	4	4
Discount Rate (%)	15	15	15
Payback period (Yrs.)	10	10	10
Equipment Resale Factor (%)	10	10	10
Equipment Life (Yrs.)	10	10	10
Office Equipment ($M)	0.1	0.1	0.1
Organizational Expense ($M)	0.1	0.1	0.1

Material Cost

First year material costs are taken from data presented in appendix A. Material costs for other years are this value adjusted for inflation.

Material Overhead

Material overhead represents the cost associated with material scrap, consumables that are directly tied to material use, and purchasing. Material overhead is listed as a percentage of direct material costs. Material overhead was set at 10% for the two low-production rates and 5% for the high rate.

Direct Labor Rate

Direct labor rate is the average hourly wage for the laborers and technicians who directly participate in the manufacture of the hardware. A rate of $9.00 per hour was selected based on our agreement with SAIC. This value is, in general, consistent with our experience.

Labor Burden

Labor burden is the additional cost of labor above the direct labor rate. Labor burden includes unemployment insurance, workers compensation, company social security contributions, health and medical insurance, and pension funds. It includes costs of vacations, holidays, premiums, and other fringes. First level supervision and production related engineering is included as labor burden. Facilities and maintenance related costs are included. Labor burden is ex-

pressed as a percentage of direct labor costs. Labor burden for production rates of 500, 1000 and 10,000 were assumed to be 70, 70, and 50%, respectively. This assumption is common with SAIC.

Research and Development (R&D)

R&D represents the cost associated with maintaining the technical superiority of the product. This includes engineering, technician, and associated material costs. R&D is a percentage of the gross sales. R&D was assumed to be 3% at all production rates.

General and Administrative (G&A)

G&A includes marketing, administrative, and clerical costs. G&A is listed as a percentage of the sum of the costs of direct labor, labor burden, shipping, and R&D costs. Material and material overhead is not included. G&A would be dependent on production rate. Rates of 35, 25, and 15% were assumed for production rates of 500, 1000, and 10,000 respectively.

Capital Depreciation Schedule

The tangible investment in capital (equipment costs) to initiate this manufacturing business will depreciate. A straight line depreciation schedule of seven years was assumed. Seven years is the minimum allowed by law. This is a common assumption with SAIC.

Federal Income Tax

This represents the federal income tax on corporate profit and is shown as a percentage of gross profits. Thirty-four percent was used.

State Income Tax

This represents the state income tax on corporate profit and is shown as a percentage of gross profits. Although Texas has no income tax, it was assumed that this manufacturing facility would be in a state with a 4% income tax. The combined tax (federal and state) of 38% is common with that used by SAIC.

Inflation Rate

This is the rate at which materials and labor increase in cost. It is expressed as a percentage per year. Four percent was assumed for this work. This assumption is common with SAIC.

Discount Rate

The discount rate is the rate of return of the investment (combined investment of capital and organizational expense). The discount rate is the interest rate earned on the unrecovered investment such that the unrecovered investment is zero at the end of the life of the investment. The life of the investment was assumed to be 10 years. A discount rate of 15% was selected based on Solar Kinetics' perception of what would be required to obtain investors. The present value (PV) reflects this rate. This assumption is common with SAIC.

Equipment Resale Factor

The manufacturing and office equipment will have some tangible value at the end of its life. It was assumed that the equipment would have a resale value of 10% of its original cost, adjusted for inflation. The gains from this sale are shown in year 11. This assumption is common with SAIC.

Manufacturing Equipment

Details for the manufacturing equipment costs are shown in earlier figures. Office equipment was assumed to be $100,000.

Organizational Expense

Organizational expense covers the cost of business initiation. Included in this cost are legal fees and salaries and other miscellaneous costs. An organizational expense of $100,000 was assumed.

Based on these assumptions, the price for the facet is defined by that which makes the present value of the investment greater than the initial investment. The resulting facet prices (including controls) for production rates of 500, 1000, and 10,000 facets per year are $115.00, $93.30, and $55.40 per square meter, respectively. The cost analysis spread sheets are provided in appendix C.

Figures 9.1 and 9.2 show the sensitivity of the predicted facet price to changes in the assumptions. The value of each assumption was increased 10% (one at a time), and the resulting increase in facet price was recorded. Figure 9.1 is for a production rate of 500 facets/yr, and Figure 9.2 is for 10,000 facets/yr. At high production rates, the facet cost is most sensitive to the direct material cost. The cost of tooling and operations is amortized over many facets. At lower production rates, the sensitivity to direct material costs decreases, but is still significant.

Tables 9.4 and 9.5 summarize the assumptions and facet cost. The format for these two tables is common with SAIC to facilitate cost comparisons.

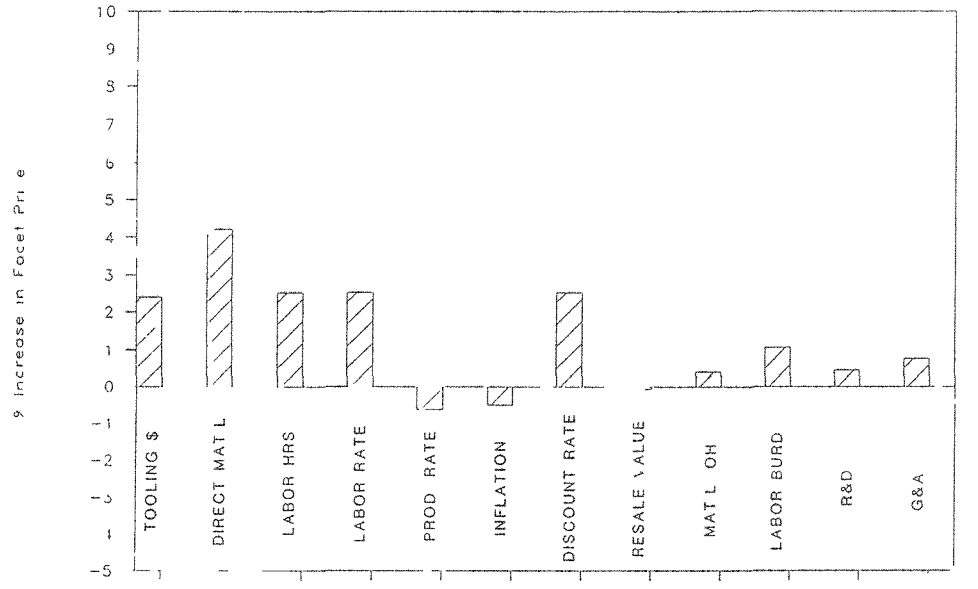

Figure 9.1 **Facet Cost Sensitivity to Key Assumptions with Production Rate of 500 Facets/Yr. Impact of a 10% Increase in the Value of the Assumptions Shown.**

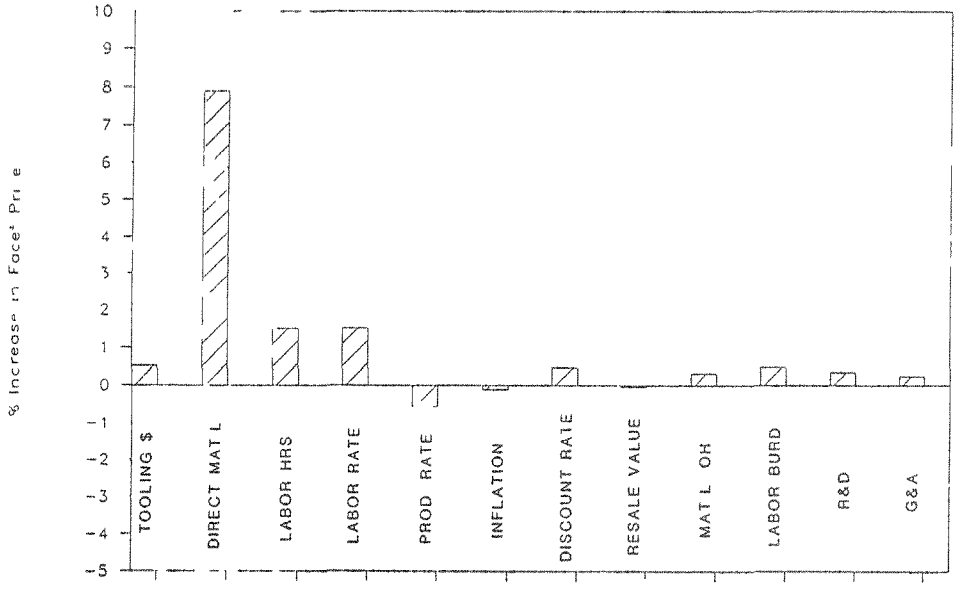

Figure 9.2 **Facet Cost Sensitivity to Key Assumptions with Production Rate of 10,000 Facets/Yr. Impact of a 10% Increase in the Value of the Assumptions Shown.**

Table 9.4
Summary of Assumptions

Common assumptions with SAIC:	
Direct Labor Rate	$9.00/hr.
Labor Burden	70% @ 500 units/yr. 70% @ 1000 units/yr. 50% @ 10000 units/yr.
Equipment Life	10 year
Equipment Salvage Value	10%
Capital Depreciation Period	7 Years
Inflation Annual	4%
Discount Rate	15%
Payback period	10 Years
Taxes (Federal and State)	38% of Profit
Direct Material Costs	
ECP-305	$2.00/ft^2
Paint	$10.00/facet
Other direct material costs based on vendor quotes and engineering estimates.	
Other Assumptions:	
Material Overhead	10% @ 500 units/yr. 10% @ 1000 units/yr. 5% @ 10000 units/yr.
R & D	3% of sales
G & A	35% @ 500 units/yr. 25% @ 1000 units/yr. 15% @ 10000 units/yr.
Office Equipment	$100,000
Organizational Expense	$100,000

Table 9.5
Cost Summary

	Annual Production Rate		
	500	1000	10000
Film Cost ($/Facet)	214.00	214.00	214.00
Other Direct Material Cost ($/Facet)	208.00	204.00	190.00
Direct Labor Hours (MnHrs/Facet)	13.60	13.60	5.20
Tooling Costs ($M)	0.63	0.63	1.33
Price, ($/Facet)	1,157.00	938.00	557.00
($/m^2)	115.00	93.30	55.40

10.0 PROTOTYPE DEVELOPMENT

Two prototype facets were made during this contract. The objective for making and testing these facets was to demonstrate high optical quality and soundness of the design while discovering and overcoming design and construction subtleties. The first facet was successful, having a slope error between 2.0 and 2.3 mrad for the range of focal lengths measured. Its control system was not representative of the commercial controls. The second facet used the ring and rear membrane of the first along with a new front membrane. Its control system was representative of the commercial unit. The accuracy improved to a range of 1.1 to 1.4 mrad.

This section of the report discusses the development of these two facets. The similarities between the prototypes and the commercial unit are addressed, followed by a discussion of the technique used to construct the prototypes. Finally, the results of optical testing are presented and evaluated.

10.1 COMMERCIAL AND PROTOTYPE COMPARISON

The prototype facets closely represent the commercial unit. Some unavoidable differences exist in such areas as alloy type and control system components. A comparative summary is provided in Table 10.1. The cross section of the ring is identical. Cor-Ten was used in place of low carbon steel for the ring. Cor-Ten is a corrosion resistant carbon steel with a yield strength of 50,000 psi. The prototype ring was made in four sections to allow looser tolerances on the prototype ring bending process. The commercial ring will be one piece with one butt joint.

The front membrane of the prototype is identical to that of the commercial unit. The prototype rear membrane is the same thickness as the commercial one, but is fully annealed rather than one-quarter hard. The process and hardware to attach the prototype membranes to the ring differed slightly from the commercial process. The cross section of the clips was identical to the commercial design as was the clip material. The prototype clips were made into discrete sections, each four inches long. The commercial design calls for a continuous clip. This difference was required to avoid the tooling costs required to make and install continuous clips.

The tether hardware differed from the commercial design only slightly. The prototype disks that capture the front membrane were machined rather than injection molded. The access plate and mating flange were off-the-shelf products reinforced for use with the prototype. These parts would also be injection molded for commercial production.

Table 10.1
Prototype and Commercial Comparison

	Commercial	Prototype
Ring		
Size (inches)	8x2x.120	8x2x.120
Material	Low Carbon	Cor-Ten
Sections	1	4
Front Membrane		
Thickness (inches)	0.003	0.003
Material	304 Annealed	304 Annealed
Reflective Material	ECP-305	ECP-305
Rear Membrane		
Thickness (inches)	0.004	0.004
Material	304 1/4 Hard	304 Annealed
Clips	Continuous	Discrete
Material	301 1/2 Hard	301 1/2 Hard
Tether		
Disks	Molded	Machined
Access Plate	Molded	Off-the-Shelf
Controls		
Operational Switch	Mech. Switch	Switch/gage Combo
Over Press Switch	OEM Switch	Mech. Switch
Blower	Universal	Brushless
Weight	11.7 kg/m^2 2.4 lbs/ft^2	11.7 $kg\backslash m^2$ 2.4 lbs/ft^2

The control system used on the second facet follows the commercial design in function, but many of the components differ. The commercial pressure switch was replaced with a pressure switch/gage combination so that the set points could be easily adjusted for the three desired focal lengths. The repeatability of the gage/switch combination is better than the switch, but both are better than required (.001 psi for gage/switch and .002 psi for gage). The over-pressure switch used in the prototype is a conventional diaphragm switch. This was used in place of the original equipment manufacturer (OEM) switch specified for the commercial unit based on availability. The commercial blower is a centrifugal type powered by a universal motor. These motors have a limited operating range with respect to flow rate and pressure. A brushless DC motor was selected for the prototype to ensure a wide operating range. A centrifugal blower was used. The solenoid valve selected for the prototype differed from the commercial valve only in size. A large orifice valve was selected to ensure adequate flow for the prototype. The enclosure and miscellaneous wiring used on the prototype were unique to the prototype.

10.2 CONSTRUCTION TECHNIQUE

The facets were made in a similar fashion to heliostats and the single-element dish (Refs. 5 and 3). Much of the tooling was the same. Several new techniques and tools were required.

The ring was made from flat sheet stock. A steel fabricator sheared the sheet and formed the flanges using a press brake. The straight ring sections (3.7 m (12 feet) long) were formed into curved sections at SKI using modified pyramid rolls. Collars on the rollers were used to prevent the flanges from splaying. The ring sections were cut to length and were jigged for welding in a ring fixture that was later used for membrane testing and for the remainder of facet construction. The ring was welded, and its planarity and roundness were assessed. The ring was planar within +/- 0.5 mm (+/- 0.02 inches) and was round within 4.1 mm (+/- 0.16 inches) as measured to the line of departure of the front membrane at eight locations. The ring was removed from the fixture and sandblasted where the clips attached.

After sandblasting, the ring was returned to the fixture with the rear side up for installation of the rear membrane (Figure 10.1). The membrane was supported on the ring, and a series of weights was attached to its perimeter. The load from the weights was insignificant in terms of membrane tension; they were used only to remove slack from the membrane. The weights induced 160 N/m (0.9 pounds/in) tension. A bladder between the ring and the tooling was inflated to roll the top of the ring inward (Figure 10.2). The membrane was then clamped to the ring. When the bladder load was removed, the ring sprung back and induced tension in the membrane. The membrane was clamped to the ring using discrete clamps and rolled bar stock to distribute the clamping load. Figure 10.3 shows these clamps in use. Reflections of the ceiling and lamps can be seen in the membrane. These clamps were used on the rear membrane because they are easily removed and allow several corrective iterations to improve the membrane installation technique. Once the membrane was properly installed, the bladder was reinflated and the tooling clips were replaced with facet clips. The membrane was tack welded to the ring periodically to ensure the action of forcing the clips on would not cause relative motion between the membrane and ring. The installed rear membrane is shown in Figure 10.4. The membrane tension was measured by placing weights in the center of the membrane and recording center deflection. This indicated that the initial tension of the rear membrane was approximately 5300 N/m (30 lbs/in).

The ring and membrane were then flipped over for installation of the front membrane. The front membrane was installed in a similar manner as the rear. Weights were used

Figure 10.1 Prototype Ring Supported in Assembly Fixture.

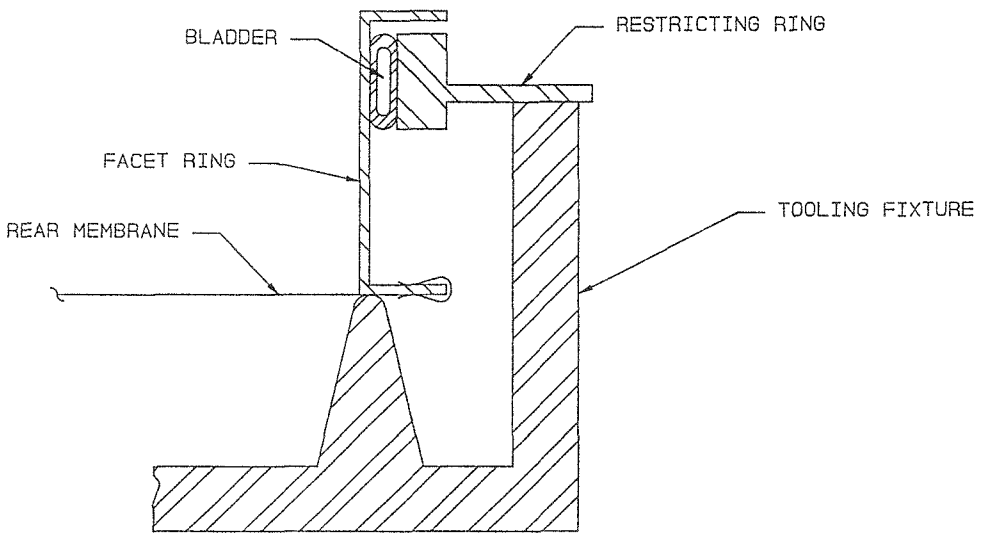

Figure 10.2 Schematic of Ring and Assembly Fixture.

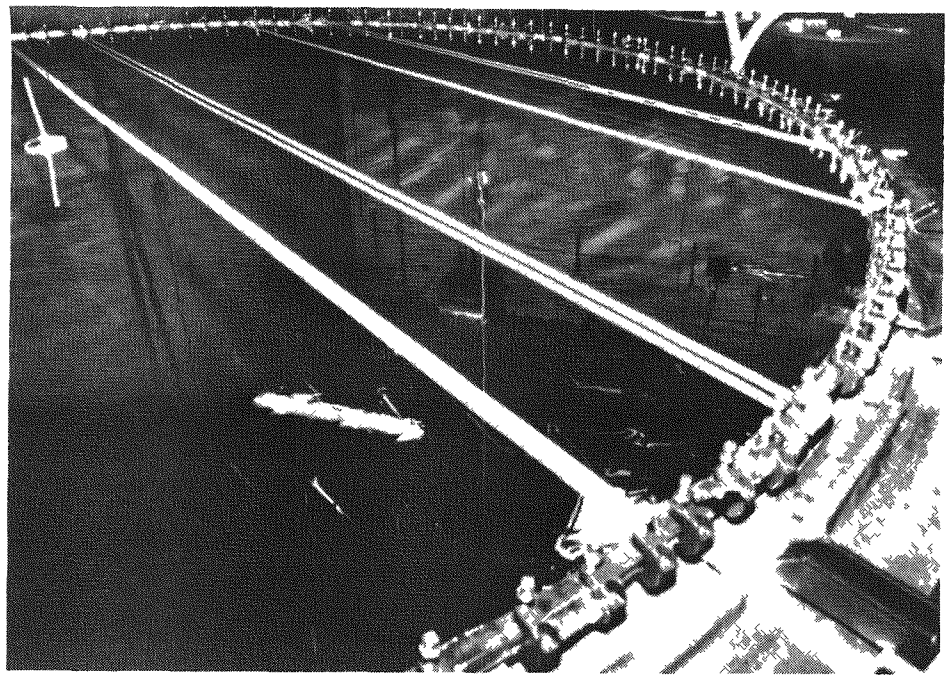

Figure 10.3 Membrane Clamps Used During Prototype Assembly.

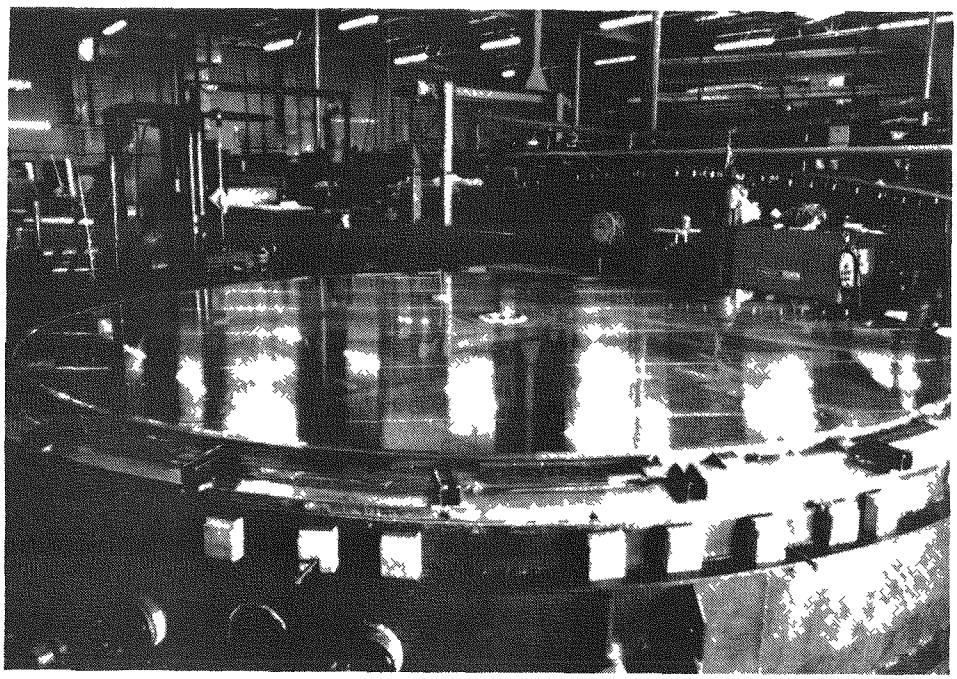

Figure 10.4 Facet in Tooling Showing Installed Rear Membrane.

to remove slack, and ring roll was used to eliminate the waviness caused by excess material in the membrane. Excess material is present in the membrane due to coil stock that is not flat and from the imperfect seaming of this material. The tooling clamps were essential for the front membrane because the facet clips were not designed to hold the membrane during the high loads introduced during forming. The front membrane of the first facet was not handled well during this operation. As a result, the membrane was creased locally at many locations. This effect can be seen in the lower section of the completed facet shown in Figure 10.5.

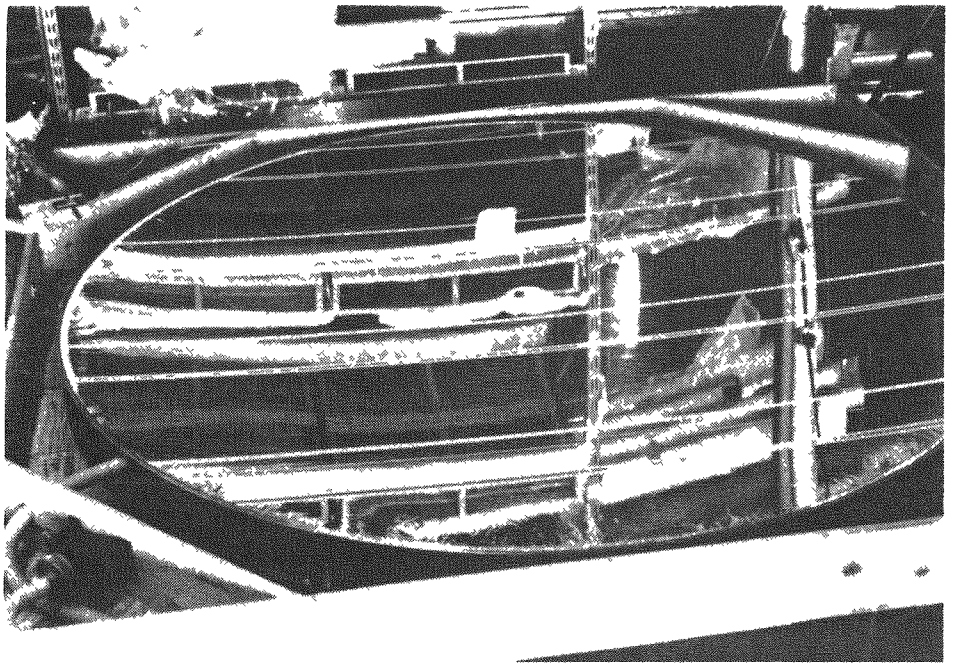

Figure 10.5 First Prototype Facet in Shipping Crate.

The front membrane was formed by incrementally increasing the vacuum in the plenum. A slight pressure in the bladder was required to close the plenum. After each incremental increase, the vacuum was lowered to 340 Pa (.05 psi) to measure the membrane center deflection. Forming was stopped when the center deflection at 340 Pa (.05 psi) reached that of a perfect parabola having a focal length of 10.5 m. The tether access plate was removed during this process so that there was no pressure load acting on the rear membrane. Figure 10.6 shows the progression of the forming. The top line represents the membrane center deflection under forming loads. The bottom line shows the corresponding deflection at 340 Pa (.05 psi).

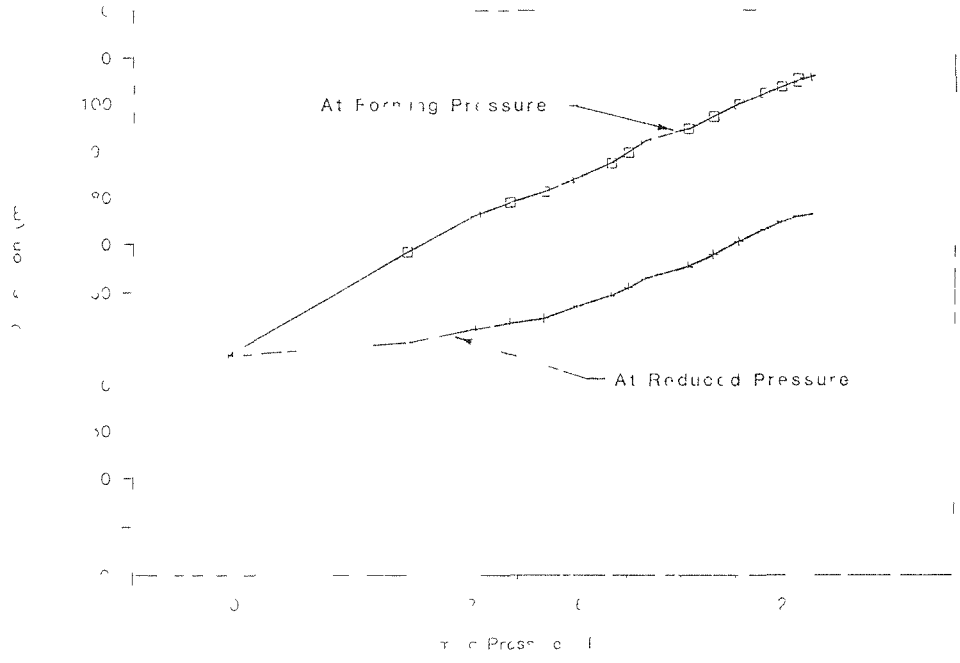

Figure 10.6 Forming Loads for First Facet.

Figure 10.7 is the measured slope error of the first facet. Two focal lengths are shown. The slope error term is the difference between the actual and the theoretical slope, where the theoretical slope is defined as that of a perfect parabola having a center deflection equal to that which was measured during the test. Iterations to determine the best-fit focal length were not performed. The shape of the curve differs from the one measured in the membrane tests. The shorter focal length has a better shape than the longer one. The membrane tests showed opposite results. There were several differences between the test membrane and the facet membrane that could contribute to such differences. The test membrane was attached to a rigid tool along its perimeter unlike the facet membrane which was attached to the relatively compliant facet ring. As the vacuum increased, the facet ring would roll and shrink, and thereby, alter the membrane shape. Other less significant differences include initial membrane tension and bladder pressure. An inflatable bladder was used to close the plenum between the tool and the facet ring. This bladder exerts a small radial pressure on the ring which could cause some ring motion that did not occur in the membrane test.

The tooling clamps were removed one at a time, and the membrane clips were installed on the front membrane. Temporary clamps and a careful technique were used to prevent relative motion between the membrane and the ring.

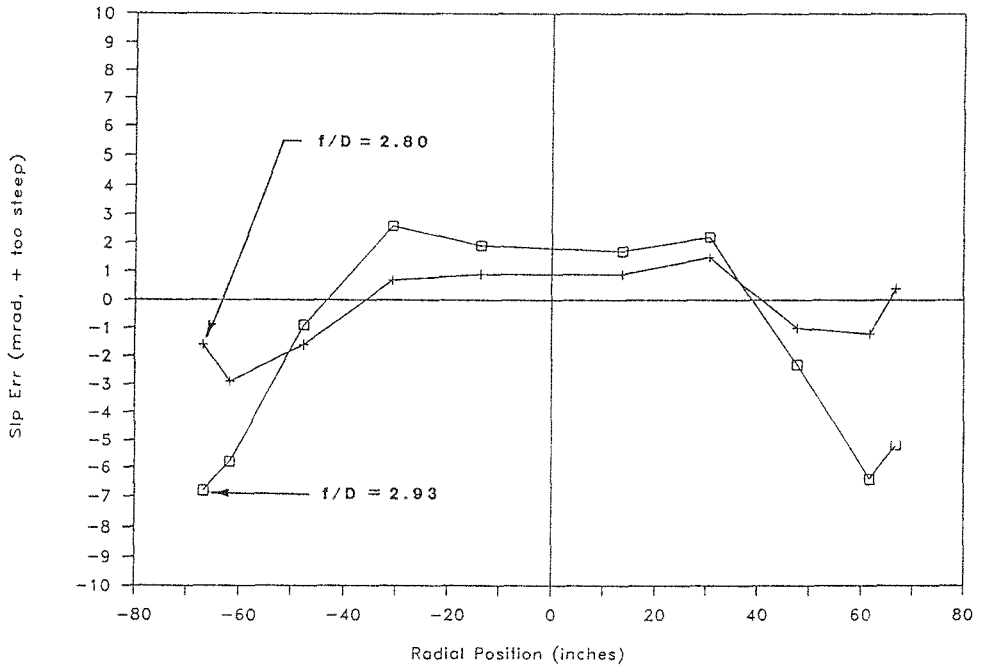

Figure 10.7 Slope Error Results of First Facet.

The facet was removed from the tooling and placed in a shipping crate. The remainder of the tether assembly (disks and rod) was then installed.

The facet, supported on six points in the crate, was then shipped to SERI for evaluation. Three additional mounting points were added just for shipment of the prototype; the other three were facet-to-dish hardware. The second facet was shipped without the three extra supports with no apparent ill effect.

The first-generation facet was returned from SERI following their evaluation. It was placed back into the fixture, and the front membrane was removed. Another membrane was installed using an improved technique. Handling-induced creases were greatly reduced. The method for attaching the weights to the membrane was improved. This prevented a problem of some weights falling off during assembly and resulted in higher and more uniform loading. The bladder was modified to reduce the magnitude of nonuniform loading caused by the joints at the two ends of the bladder.

The front membrane was formed using the same technique as used for the first facet. The membrane was then tack welded to the ring to ensure no slippage during installation of the membrane clips. It was then crated, the tether installed, and returned to SERI for evaluation.

10.3 DISCUSSION OF PROTOTYPE RESULTS

The optical accuracy of the facets as measured at SERI exceeded project goals. However, three problems became apparent from the SERI tests. The effect of these problems is not expected to be severe and a method to avoid them could likely be resolved with simple tests.

The first of the problems was that the center deflection of the second facet appeared to change from the time it was measured in Texas (SKI) to when it was measured in Colorado (SERI). At identical operational pressures, the center deflection as measured in Colorado was approximately 4 mm (0.16 inches) less than that measured in Texas. The cause of this difference is unknown, but several viable ideas have been reviewed.

The facet faced the zenith during measurements in Texas and faced the horizon in Colorado. Weight of the front membrane is small. The difference in orientation is not believed to be responsible for the change in center deflection.

The tether was damaged during shipment. The tether stop was pulled through the access plate indicating that either the front membrane pulled too hard on the stop or that the stop was pushed from behind by its shipping restraint. It is most likely that the front membrane was not involved. If the front membrane was yielded from this, the center deflections measured in Colorado would be greater than those of Texas instead of being less. Damage during shipping is not a likely cause for the difference in center displacement.

The effects of a change in temperature was expected to have some effect on the focal length. SERI aided in the investigation and measured the center deflection at two different temperatures and found no noticeable difference. This unexpected result is not understood.

The most likely cause of this abnormality is an isolated measurement error made by SKI. Repeated measurements were taken in Colorado, but only one set was taken in Texas. A single error in reading a reference mark could have caused the difference. (The Texas measurements were taken with an optical level referenced to the ring edge.)

The importance of this apparent change in center deflection is large if it is a function of orientation or temperature, but is low if it is an isolated measurement error as suspected. If it is a function of orientation or temperature, the control system would need to be modified to respond to membrane position rather than plenum vacuum.

The second problem is that the center deflection was not a good indicator of the focal length of the second facet. The focal length, calculated based on a perfect parabola with the measured center deflection, was between 0.15 and 0.3 meters shorter than the best fit focal length based on SERI's measurements of the surface contour with their SHOT system. The cause of this difference could be due to the shape variation from a

true parabola; but with accuracies better than two mrad, this does not seem likely. It could be due to inaccuracies of the center deflection measurements, but it is unlikely that the inaccuracies of the SERI measurements were as high as 0.09 inches, which would account for the difference. The significance of this difference is low if it is consistent from one membrane to the next. No comparisons could be made with the first facet because reliable center deflection measurements were not made.

The third problem has to do with repeatability of the forming process. The operational pressure required to achieve the desired focal lengths was different for the two facets. The desired focal lengths range from 9.5 to 10.5 m. The first facet produced these focal lengths with pressure from 320 to 570 Pa (0.046 to 0.082 psi), respectively. The second facet required 640 to 990 Pa (0.093 to 0.143 psi) to cover the focal length range. This suggests that the membranes were formed differently. This is important if a group of facets are ganged under one pressure controller.

The most likely cause of this difference between first and second generation facets is the change in the facet assembly procedure made for the second facet. The most significant change is the method used to install the 113 membrane clips on the front membrane. The technique used to install the clips on the first prototype relied heavily on technician skill to keep the membrane from moving relative to the ring. The membrane is formed prior to clip installation, and any change in position would alter the shape. The membrane for the second facet was tack welded to the ring to ensure no relative motion during clip installation. If the membrane on the first facet slipped relative to the ring, it would explain the differences in focal lengths. This motion, however, would have to be consistent from one clip to the next, or the shape of the membrane would be worse than it was (2.0 to 2.3 mrad). Another difference between techniques is that greater tension was used on the front membrane of the second facet during fixturing and prior to forming. This was achieved by using more edge weights during installation. The effect of this is not expected to be large because the pressure required to form the membranes was consistent. This will be discussed later in this section. The bladder used to compress the ring during installation was also altered. The change was a local improvement of joint at the ends of the hose and is not considered to have caused this difference. Any of these assembly process changes could have contributed to the change in focal length. None is significant, because process changes would not reoccur during production.

An unknown or uncontrolled forming or assembly variable could have caused this third problem. If so, this variable must be identified and controlled.

Some facet operational variable may have caused the difference between the two facets. Temperature or humidity (reaction with the polymer film) conceivably could have caused the difference. This appears unlikely based on SERI's temperature tests of the second facet and because of the low structural stiffness of the polymer film.

An additional potential cause of the difference between the two membranes is a measurement error during forming. Such an error could cause the membrane to be

under or over formed. This is unlikely because the pressure required to form each of the membranes was almost identical. It is possible that an error in the measurement of center deflection during forming would result in an apparent difference between the two membranes. Figure 10.8 shows the center deflection of each membrane as a function of the forming pressure. The two membranes followed each other very closely. Figure 10.9 shows the deflection under operational pressure as a function of forming pressure. There are only slight differences apparent.

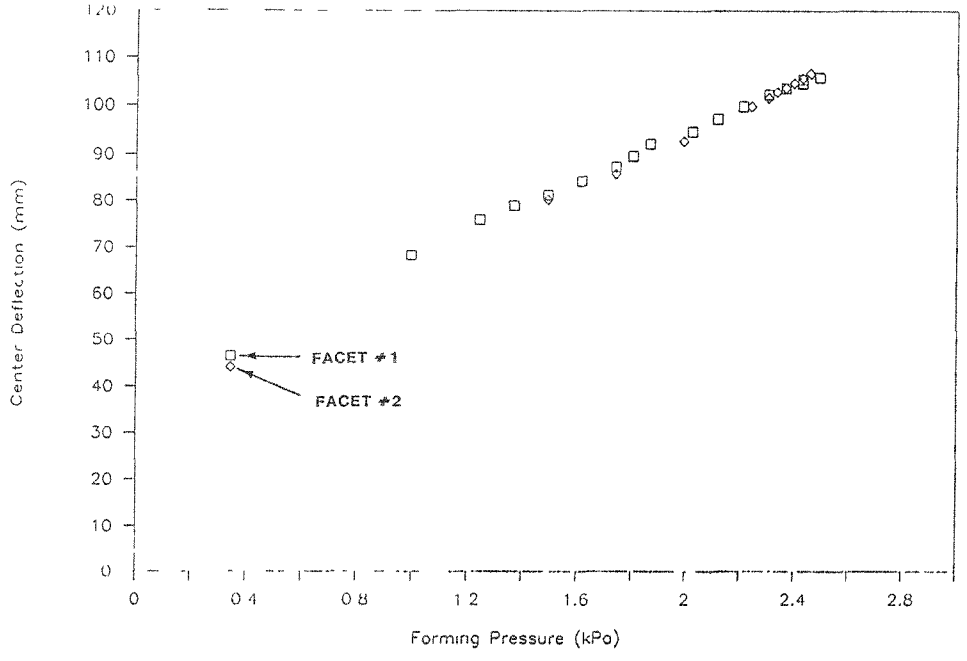

Figure 10.8 Center Deflection at Intermediate States of Forming (at Forming Pressure).

It seems most likely that the front membrane slipped on the ring during installation of the first membrane, but this cannot be proven.

If the focal length difference is caused by a variable of the forming or assembly process that is difficult to control, each facet would require its own solenoid valve and set of pressure switches. This would increase the price of the facet by 8% at the low production rate and 11% at the high rate.

The fact remains that the first facet met the slope error goal of this contract of 2.5 mrad, and the second facet far exceeded it having a slope error as low as 1.1 mrad. Table 10.2 presents the measured slope error of each of the facets over the range of focal lengths tested.

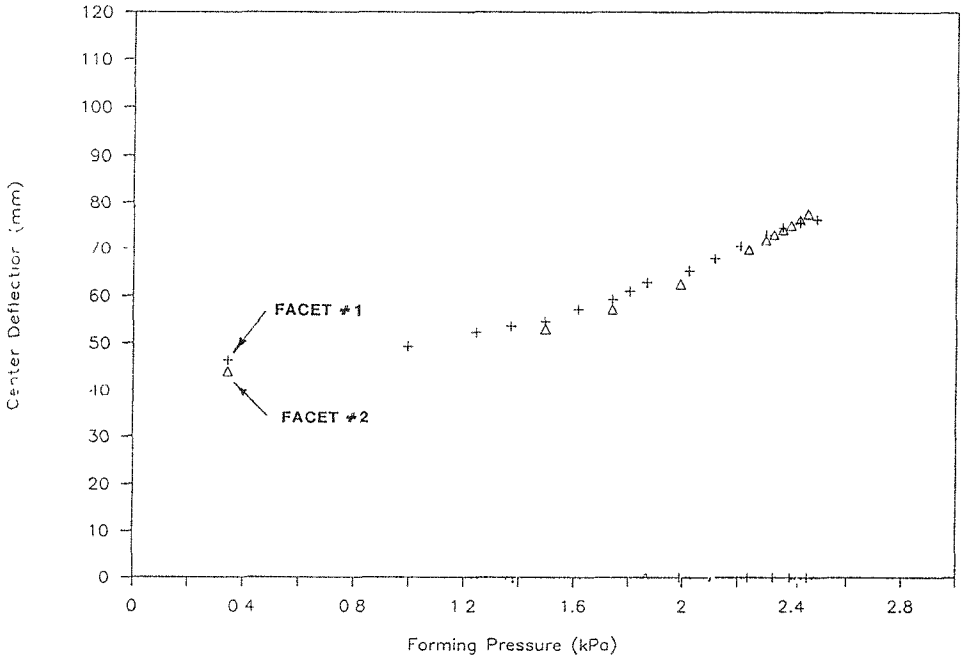

Figure 10.9 Center Deflection at Intermediate States of Forming (at Operational Pressure).

Table 10.2
Equivalent Slope Error as Measured by SERI

Facet #1		Facet #2	
Focal Length (m)	Error (mrad)	Focal Length (m)	Error (mrad)
9.70	2.15	9.45	1.30
10.10	2.05	9.85	1.15
10.50	2.35	10.40	1.45

SERI measured the contour of each facet over the intended range of focal lengths (Ref. 18). They used a laser scanning system called SHOT. This system directs a thin laser beam to the facet from a source located near the center of the membrane's radius of curvature. This beam is reflected back to a target and it's strike location is recorded. The geometry of the incident and reflected beam allows the determination of surface slope. Each facet was scanned at approximately 2000 locations. The data is compared to a perfect parabola to define RMS slope error. Figure 10.10 shows errors of the first facet at a focal length of 9.7 m. The image represents the frontal view of the membrane surface. The lines are vector representations of the slope error showing both location and magnitude. A scale bar of 1.67 mrad is shown on the right. Considerable scattering is evident near the perimeter. This is caused by the handling damage and local waviness

where the membrane was slack. Figure 10.11 is a similar image of the second facet with 9.45 m focal length. The crosses represent strike locations. The lines represent direction and magnitude of slope error. Substantial improvements are evident near the perimeter of the membrane where scatter has been reduced. All slack areas were removed from the second facet, and the membrane handling was much improved. The magnitude of all vectors was reduced. The RMS slope error was reduced from 1.67 to 1.14 mrad for the shortest focal lengths.

The slope departs from a perfect parabola in a systematic manner, and therefore, an RMS slope error term may not be an accurate indicator for determination of optical performance. To address this, SERI compared the image size (at the focal plane) that would be generated by the facet to that of a perfect parabolic reflector with some random, normally distributed error. The error that gives an equivalent spot size is defined as the equivalent slope error of the facet. The equivalent slope error for the facets as a function of focal length is shown in Figure 10.12. The best shape occurs at the mid range focal lengths and is 2.05 mrad for the first facet and 1.15 mrad for the second.

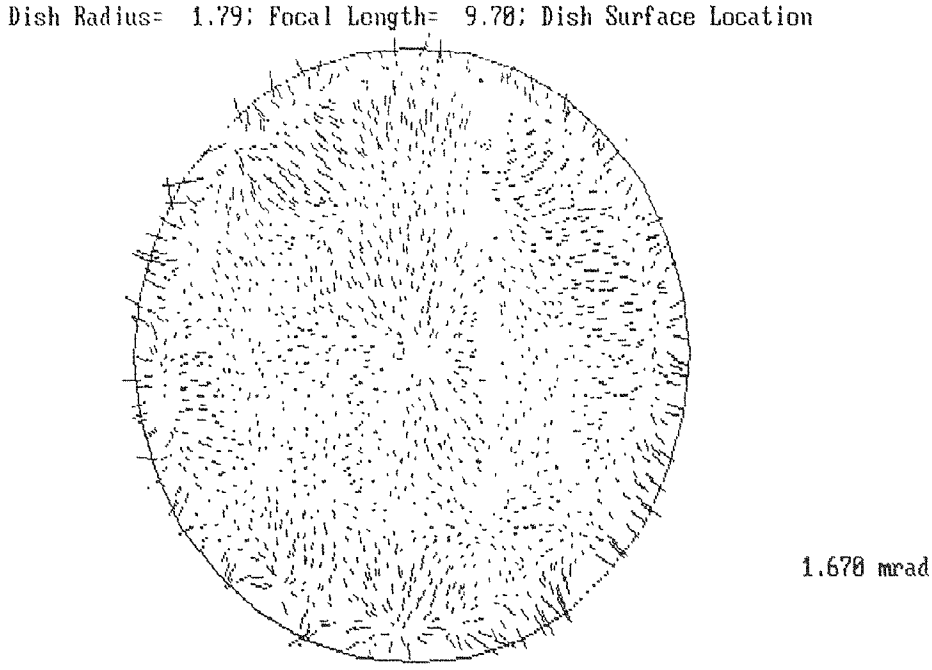

Figure 10.10 Slope Errors of First Facet as Measured by SERI.

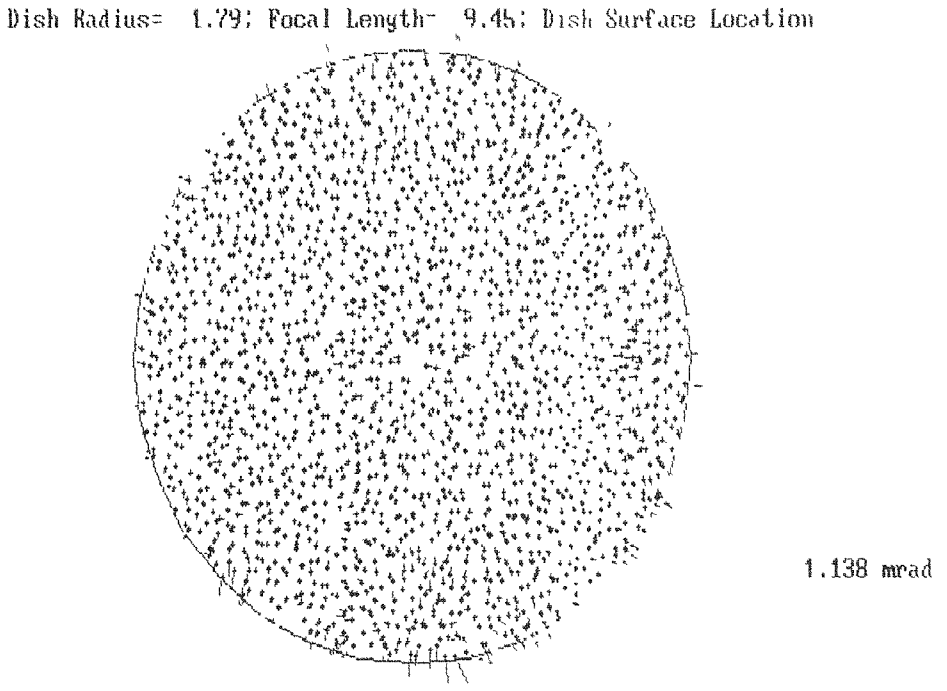

Figure 10.11 Slope Errors of Second Facet as Measured by SERI.

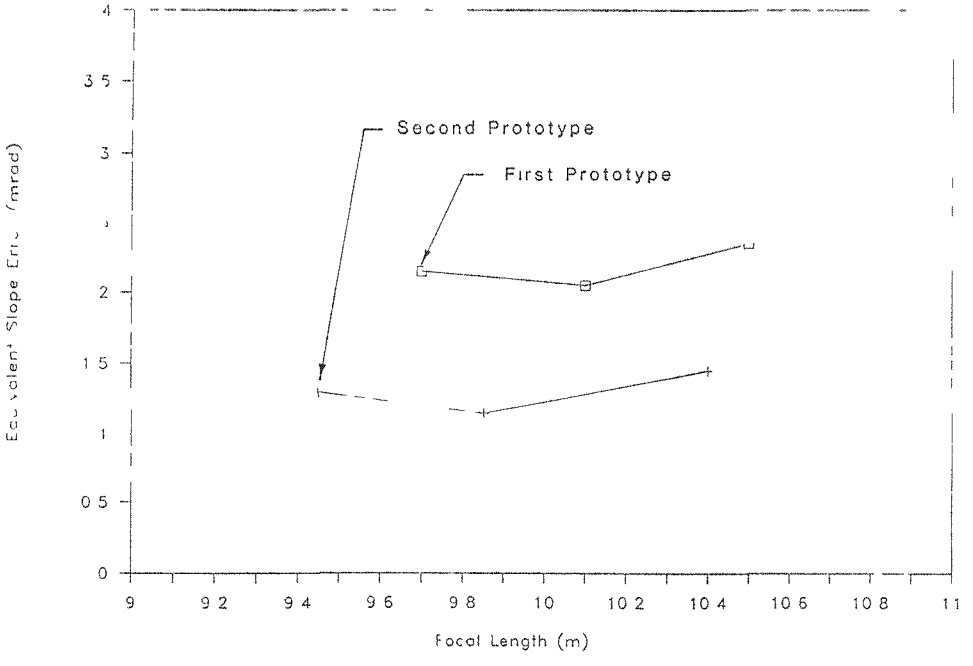

Figure 10.12 Equivalent Slope Error as Measured by SERI (Ref. 18).

11.0 RECOMMENDED FUTURE WORK

The completion of a design and prototype effort offers a perspective on the product in terms of its capabilities and limitations. This perspective points out the need for additional work on some items.

Since the second facet exists, it would be advantageous to poke and prod it and learn what we can. Three tests should be done on the existing facet to help confirm the design:

* The ability of the tether to restrain the front membrane in the wind should be tested. This ability has been assumed and not confirmed.

* The effect of the oscillating wind on the real-time optics should be tested and compared with the analysis that indicates it will be small. This test would require the facet to be removed from its shipping crate or the rear face of the crate to be removed so the crate does not alter the response.

* The facet should be operated in the extreme cold to confirm its ability to survive the anticipated high stresses.

More tests can be done on the existing facet to address the problems in facet focal length and center deflection:

* The center deflection should be measured with respect to facet orientation to remove this as a possible source of the difference between measurements in Texas and Colorado. Measurement of facet performance as a function of orientation would not be needed unless the center deflection measurements indicated a sensitivity.

* The facet should be returned to the assembly tooling, and the center deflection measured under the conditions of assembly. This will clarify how the tooling affects the center deflection and define how the deflection achieved during forming represents the final center deflection.

* The next few facets should be built with rigorous control of all variables to confirm repeatability. The first two facets were made with different techniques and repeatability of the forming process could not be established.

The interaction of the facet with the dish system needs more complete evaluation:

* A more rigorous analysis of the performance penalty of ganging facets for focus control should be evaluated. The effect is believed to be small based on an initial review using equivalent slope error as a figure of merit. A more detailed analysis with an optical code is warranted.

* A realistic budget for receiver limitations needs to be developed. This budget should define allowable focal length deviation from ideal for a facet. This

impacts the facet design in terms of facet ganging and operational pressure deadband. The acceptability of wind induced focal length transients also needs to be established with respect to magnitude and duration.

Three design changes have the potential to reduce the facet cost or improve its reliability:

* Passive pressure regulators better suited for this application should be tested on the current prototype. If successful, these regulators would replace electro-mechanical parts of the focus control system with passive devices.

* Focal length control by sensing the position of the front membrane should be reconsidered as an option to avoid sensitivity to operational and manufacturing variables.

* The issues concerning welding the membranes to the ring should be reviewed. Welding has the potential to eliminate the need for attachment clips and reduce the facet weight and cost.

The existing facet could be used in one more test that could benefit SKI, SANDIA, and SERI in a larger context than facet development.

* The facet should be measured with SKI's VRT measuring system. The results of this measurement should be compared with the results from SERI's measurements with the SHOT system and SANDIA's measurements with the BCS. This opportunity for a one-to-one comparison is rare and would help validate each of the three measuring systems. The results would also be useful to SKI for comparison with future facets.

12.0 SUMMARY

An optical facet for a faceted-membrane dish has been designed and successfully demonstrated. The faceted stretched-membrane dish, which Sandia National Laboratories is developing, will require twelve of these facets. Each of the twelve facets are identical. The facet and associated focus control system has been designed and demonstrated at full scale. Facet accuracy of 1.1 mrad was achieved, which well exceeded the goal of 2.5 mrad. Facet weight is desirably low at 119 kg (261 lbs) which is 11.7 kg/m^2 (2.4 lbs/ft^2).

The facet is similar to a stretched-membrane heliostat in that it has a ring and two membranes, but there the similarities end. The front membrane is plastically formed to a concave shape and is stabilized during stow by a passive tether. This tether pulls the center of the front membrane to the rear when the operational pressure is removed. Figure 12.1 shows a prototype facet with the tether engaged. The ladder on the left provides scale for the 3.6 m diameter facet. The operational pressure (a slight vacuum in the plenum) is provided to stabilize the membrane during operation and to achieve the desired focal length ranging from 9.5 to 10.5 m. A centrifugal blower provides the pressure that is controlled by pressure switches. Figure 12.2 shows a facet under operational pressure.

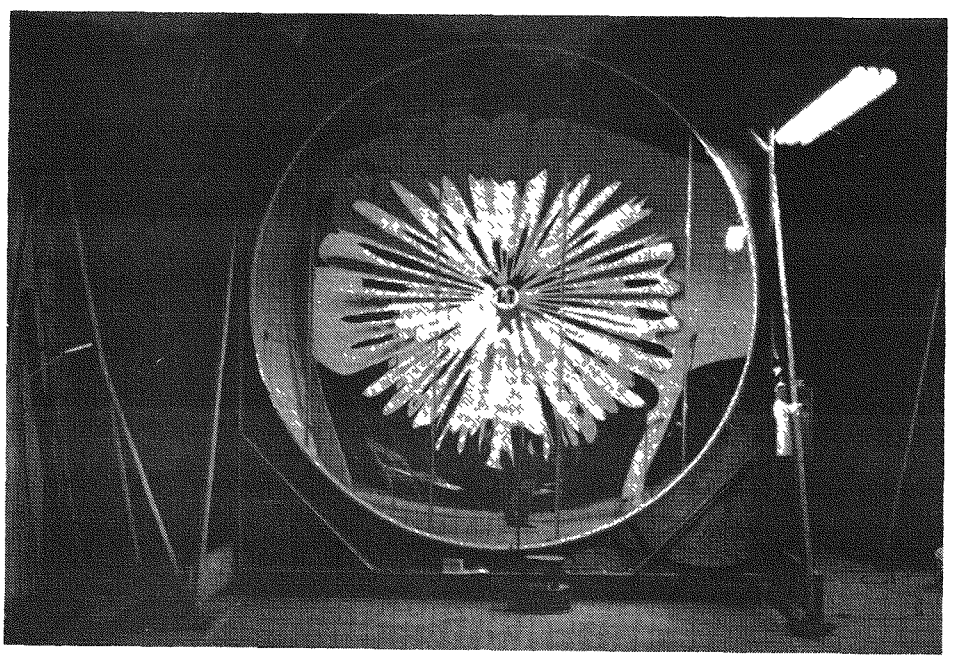

Figure 12.1 Second Prototype Facet Stabilized with Passive Tether.

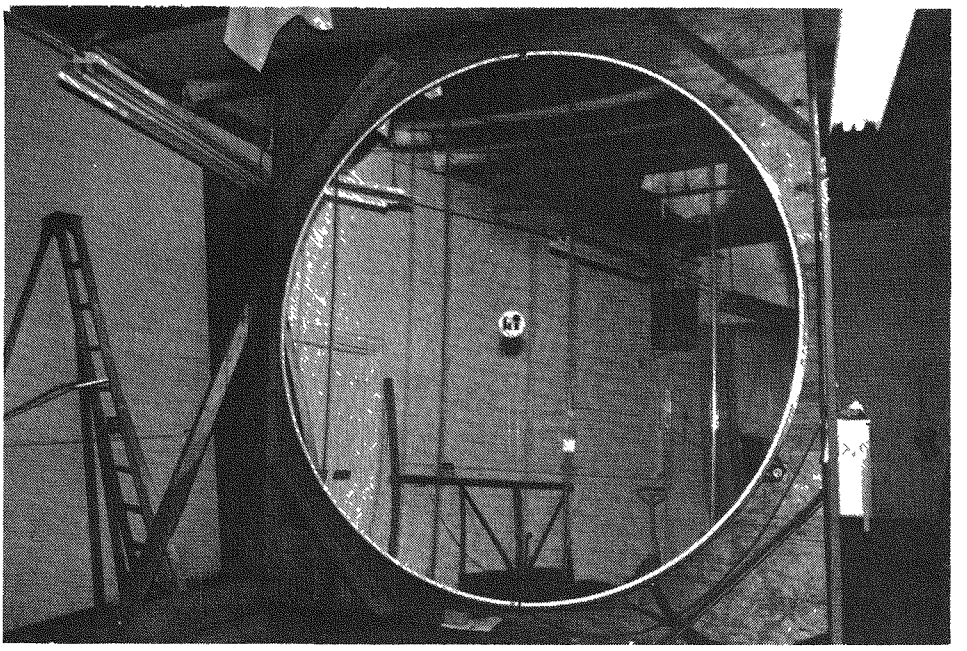

Figure 12.2 Second Prototype Facet During Operational Testing.

Original concepts for this facet were simply scaled versions of stretched-membrane heliostats with fully elastic membranes. However, the original specifications for small f/D's forced the departure to plastically formed front membranes. The specifications were later relaxed, but the benefits of low ring weight and high optical accuracy were still maintained with the plastic membrane approach.

Fundamental issues associated with this approach were resolved early in the contract with tests on membranes alone. We found that the reflective laminate (specifically 3M's ECP-305) survived the forming process, and that the stress concentrations induced by the ECP seams did not cause metal rupture, and most importantly, that accurate contours could be achieved.

The ring was sized based on stress and will have almost no deflection during operation. It represents 62% of the facet weight, but is made from low-cost carbon steel sheet metal. The membranes are made from stainless steel, the front being 0.08 mm (3 mils) thick and the rear being 0.10 mm (4 mils) thick.

Two prototypes were built, the second prototype using the ring and rear membrane of the first. Each facet weighed 11.7 kg/m^2 (2.4 lbs/ft^2) and each exceeded the accuracy goals with the second facet being better than the first by about one mrad.

Slight differences were observed between the focal lengths of the first and second facet, but were likely caused by planned differences in the assembly procedure. Some differences were also noted between center deflection measurements taken at SKI and those taken at SERI. The differences were likely caused by a SKI measurement error.

A study was done to estimate the cost to commercially manufacture this facet at various production rates. Results indicate that the facet can be sold for $\$115/m^2$ at a production rate of 500 facets per year and $\$55.40/m^2$ at a rate of 10,000 facets per year. As with many mass-produced manufactured goods, the raw material costs are the largest component of the manufacturing cost. The reflective film represents over 50% of the raw material cost. The low ring weight helps keep the total facet cost low.

13.0 REFERENCES

1. L. M. Murphy, Moderate Axisymmetric Deformations of Optical Membrane Surfaces, SERI/TP-253-3020, Golden, CO: Solar Energy Research Institute, February 1987.

2. L. M. Murphy and C. Tuan, The Formation of Optical Membrane Reflector Surfaces Using Uniform Pressure Loading, SERI/TR-253-3025, Golden, CO: Solar Energy Research Institute, August 1987.

3. Development of a Stretched-Membrane Dish-Phase I, SAND88-7035 (Solar Kinetics, Inc., Dallas, Texas), Albuquerque, NM: Sandia National Laboratories, March 1989.

4. T. Mancini, Sandia National Laboratories, Letter for Distribution dated March 9, 1990.

5. Design and Demonstration of an Improved Stretched-Membrane Heliostat, SAND89-7028 (Solar Kinetics, Inc., Dallas, Texas), Albuquerque, NM: Sandia National Laboratories, December 1989.

6. D. J. Alpert, R. M. Houser, A. A. Heckes, and W. W. Erdman, An Assessment of Second-Generation Stretched-Membrane Mirror Modules, SAND90-0183, Albuquerque, NM: Sandia National Laboratories, February 1990.

7. SERI fax transmittal of October 23, 1990, including Hauser Laboratories Test Report 90-0343, Boulder, CO, July 19, 1990.

8. J. A. Peterka, R. G. Derickson and J. E. Cermak, Wind Loads and Local Pressure Distributions on Parabolic Dish Solar Collectors, SERI/TP-253-3668, Golden, CO: Solar Energy Research Institute, May 1990.

9. J. A. Peterka, Z. Tan, B. Bienkiwicz, and J. E. Cermak, Wind Loads on Heliostats and Parabolic Dish Collectors, SERI/STR-253-3431, Golden, CO: Solar Energy Research Institute, November 1988.

10. Mean and Peak Wind Load Reduction on Heliostats, SERI/STR-253-3212 (Colorado State University), Golden, CO: Solar Energy Research Institute, September 1987.

11. L. M. Murphy, Analytical Modeling and Structural Response of a Stretched-Membrane Reflective Module, SERI/TR-253-2101, Golden, CO: Solar Energy Research Institute, June 1984.

12. S. P. Timoshenko and J. M. Gere, Theory of Elastic Stability, 2nd ed., New York: McGraw-Hill, 1961.

13. L. M. Murphy, D. Simms, and D. V. Sallis, Structural Design Considerations for Stretched-Membrane Heliostat Reflector Modules with Stability and Initial Imperfection Considerations, SERI/TR-253-2338, Golden, CO: Solar Energy Research Institute, October 1986.

14. W. C. Young, Roark's Formulas for Stress and Strain, 6th ed., New York: McGraw-Hill, 1989.

15. "Faceted Stretched-Membrane Dish Development Project, Statement of Work," PR 42-9814, June 7, 1989.

16. K. Beninga, B. Butler, Ph.D., J. Sandubrae, and K. Walcott, An Improved Design for Stretched-Membrane Heliostats, SAND89-7027, Albuquerque, NM: Sandia National Laboratories, June 1989.

17. K. Beninga, R. Davenport, and J. Sandubrae, Selection and Design of a Stretched-Membrane Heliostat for Today's Markets, SAND89-7040, Albuquerque, NM: Sandia National Laboratories, January 1990.

18. M. Carasso, Solar Energy Research Institute, correspondence to Solar Kinetics, Inc., June 25, 1990, with attachments and subsequent report data dated November 6, 1990.

APPENDIX A
DIRECT MATERIAL COSTS

Notation in the right column denotes source of prices. Q represents a vendor quote and E represents an estimate.

Direct Material Costs
Production Rate = 500 facets per year

Description	Units	Qty	$/unit	$	% of total	
Ring low carbon	#	181	0.26	47.06	11.1	Q
Ring doubler, low carbon	#	1	0.26	0.26	0.1	Q
Rear Membrane, 304	#	19	1.308	24.85	5.9	Q
Front Membrane, 304	#	14	1.308	18.31	4.3	Q
Clips, 301	#	20	1.375	27.50	6.5	Q
ECP	sq ft	107	2	214.00	50.6	Agreement with SAIC
Tedlar Tape	sq ft	9.7	0.046	0.45	0.1	Q
FEK tape	sq ft	6.6	2	13.20	3.1	Based on ECP 305 cost
Support Brackets, A366	#	13	0.217	2.82	0.7	Q
Bracket Rods	ft	2.62	1.3	3.41	0.8	Q
Bracket nuts and washers	lot	1	3	3.00	0.7	E
Urethane washers	ft	0.433	9.482	4.11	1.0	Q on matl, inflated 10 % to account for manufact
Bracket bolts & washers	lot	1	1	1.00	0.2	E
Tether discs	#	0.5	3	1.50	0.4	E
Tether rod & hardware	lot	1	2	2.00	0.5	E
Rear Flange	ea	1	4	4.00	0.9	E
Rear Flange doubler	#	1	1.308	1.31	0.3	Q
Paint	gal	1	10	10.00	2.4	E
Total in facet envelop				378.77	89.6	

Controls for entire dish (3 gangs)			
Blower	35.00	0.7	E
Motor Control	47.00	0.9	Q
Enclosure	69.00	1.4	Q
Op Pressure switches (3)	154.00	3.0	Q
Over Pressure Switches (3)	25.14	0.5	Q
Solenoid Valves (3)	57.12	1.1	Q
Wiring and misc electric	50.00	1.0	E
Ducting and Pres sensor tubing	90.00	1.8	E
Total Controls $ per dish	527.26		
Total Controls $ per facet	43.94	10.4	
Total cost per facet	422.71	100.0	
Facet area= 10.05			
Cost per m sq	42.06		

Direct Material Costs
Production Rate = 1000 facets per year

Description	Units	Qty	$/unit	$	% of total	
Ring low carbon	#	181	0.248	44.89	10.7	Q
Ring doubler, low carbon	#	1	0.248	0.25	0.1	Q
Rear Membrane, 304	#	19	1.261	23.96	5.7	Q
Front Membrane, 304	#	14	1.261	17.65	4.2	Q
Clips, 301	#	20	1.375	27.50	6.6	Q
ECP	sq ft	107	2	214.00	51.1	Agreement with SAIC
Tedlar Tape	sq ft	9.7	0.043	0.42	0.1	Q
FEK tape	sq ft	6.6	2	13.20	3.2	Based on ECP 305 cost
Support Brackets, A366	#	13	0.214	2.78	0.7	Q
Bracket Rods	ft	2.62	1.2	3.14	0.8	Q
Bracket nuts and washers	lot	1	3	3.00	0.7	E
Urethane washers	ft	0.433	9.482	4.11	1.0	Q on matl, inflated 10 % to account for manufact
Bracket bolts & washers	lot	1	1	1.00	0.2	E
Tether discs	#	0.5	3	1.50	0.4	E
Tether rod & hardware	lot	1	2	2.00	0.5	E
Rear Flange	ea	1	4	4.00	1.0	E
Rear Flange doubler	#	1	1.261	1.26	0.3	Q
Paint	gal	1	10	10.00	2.4	E
Total in facet envelop				374.66	89.5	

Controls for entire dish (3 gangs)			
Blower	35.00	0.7	E
Motor Control	45.00	0.9	Q
Enclosure	69.00	1.4	Q
Op Pressure switches (3)	154.00	3.1	Q
Over Pressure Switches (3)	25.14	0.5	Q
Solenoid Valves (3)	57.12	1.1	Q
Wiring and misc electric	50.00	1.0	E
Ducting and Pres sensor tubing	90.00	1.8	E
Total Controls $ per dish	525.26		
Total Controls $ per facet	43.77	10.5	
Total cost per facet	418.43	100.0	
Facet area= 10.05			
Cost per m sq	41.63		

Direct Material Costs
Production Rate = 10,000 facets per year

Description	Units	Qty	$/unit	$	% of total	
Ring low carbon	#	181	0.239	43.26	10.7	Q
Ring doubler, low carbon	#	1	0.239	0.24	0.1	Q
Rear Membrane, 304	#	19	1.23	23.37	5.8	Q
Front Membrane, 304	#	14	1.23	17.22	4.3	Q
Clips, 301	#	20	1.35	27.00	6.7	Q
ECP	sq ft	107	2	214.00	53.0	Agreement with SAIC
Tedlar Tape	sq ft	9.7	0.043	0.42	0.1	Q
FEK tape	sq ft	6.6	2	13.20	3.3	Based on ECP 305 cost
Support Brackets, A366	#	13	0.171	2.22	0.6	Q
Bracket Rods	ft	2.62	1.15	3.01	0.7	Q
Bracket nuts and washers	lot	1	3	3.00	0.7	E
Urethane washers	ft	0.433	9.108	3.94	1.0	Q on matl, inflated 10 % to account for manufact
Bracket bolts & washers	lot	1	1	1.00	0.2	E
Tether discs	#	0.5	3	1.50	0.4	E
Tether rod & hardware	lot	1	2	2.00	0.5	E
Rear Flange	ea	1	4	4.00	1.0	E
Rear Flange doubler	#	1	1.23	1.23	0.3	Q
Paint	gal	1	10	10.00	2.5	E
Total in facet envelop				370.61	843.5	

Controls for entire dish (3 gangs)			
Blower	26.25	0.5	E
Motor Control	35.25	0.7	E
Enclosure	51.75	1.1	E
Op Pressure switches (3)	115.50	2.4	E
Over Pressure Switches (3)	18.86	0.4	E
Solenoid Valves (3)	42.84	0.9	E
Wiring and misc electric	37.50	0.8	E
Ducting and Pres sensor tubing	67.50	1.4	E

Total Controls $ per dish	395.45	
Total Controls $ per facet	32.95	8.2
Total cost per facet	403.57	100.0
Facet area= 10.05		
Cost per m sq	40.16	

APPENDIX B
TOOLING AND LABOR ESTIMATES

500 Rate

@ 500 facets per year, 2000 hrs per year

(2 units per day)

Process	Rate	Men	Equipment	Equip $
Ring				
Roll & Shear Chanl	7ft/min 2.5%of time	0.025	Roll Former	50000
Punch holes	6min/part 2.5%of time	0.025	Punch station	6000
Bend & trim	15min/part 6% , 2 men	0.12	Roll bender	20000
Shear Doubler	3min/part,1% of time	0.01	Shear	18000
Fixture & prep	30min/part 13%, 2 men	0.26	Fixture	12000
Weld	10min/part 4%, 2men	0.08	Welder	5000
QC	10min/part 4%, 2men	0.08	Fixture	3000
Paint	30min/part, 13%, 1 man	0.13	Paint Booth	7500
Support Hardware				
Shear & punch	10min/part, 4%, 1man	0.04	Shears & Punch (same)	
Fixture & weld	15min/part, 6%, 1man	0.06	Fix & welder	8000
Paint	6min/part,2.5%, 1man	0.025	Fixtures	2000
Assemble	6min/part,2.5%, 1man	0.025	Fixtures	2000
Front Membrane				
Laminate	5ft/min,5%, 3men	0.15	Laminator line	85000
Seam weld & trim	60min/part, 25%, 2men	0.5	Welder & fix	60000
			Mandrels (20)	10000
Rear Membrane				
Shear doublers	15min/part, 6%, 1 man	0.06	Power Shear	3000
Seam Weld & trim	60min/part, 25%, 2men	0.5	Welder & fix	60000
Install Doubler	15min/part, 6%, 1man	0.06	Fixture	2000
			Mandrels (20)	10000
Clips				
Slit	10ft/min,.5%, 1 man	0.005	Uncoiler & Slitter	26000
Punch	6min/part, 2.5%,1man	0.025	Punch	10000
Roll Form	6min/part, 2.5%, 1 man	0.025	Roll former	30000
Assemble				
Fixture ring	10min/part, 4%, 2men	0.08	Fixture & misc tooling	80000
Install & clip rear mem	40min/part, 17%, 2men	0.33	Clip tool	50000
Install frnt memb	40min/part, 17%, 2men	0.33		
Form, QC, Clip	30min/part,12.5%,2men	0.25	QC Tooling	8000
Install flange & tether	10min/part, 4%, 1 man	0.04		
Install control interfa	10min/part, 4%, 1man	0.04	Fixture	1000
Mount on racks	15min/part, 6%, 2men	0.12		
Control box assy	90min/12, 1.5%, 1man	0.015	Fixture	2000
Misc				
			Forklift	15000
			Overhead trolley	20000
			Shipping racks	0
			Other	25000
	Sum	3.41		630500
	Hrs/part	13.64		

1000 Rate

@ 1000 facets per year, 2000 hrs per year

(4 units per day)

Process	Rate	Men	Equipment	Equip $
Ring				
Roll & Shear Chanl	7ft/min 5%of time	0.05	Roll Former	50000
Punch holes	6min/part 5%of time	0.05	Punch station	6000
Bend & trim	15min/part 12% , 2 men	0.24	Roll bender	20000
Shear Doubler	3min/part,2% of time	0.02	Shear	18000
Fixture & prep	30min/part 25%, 2 men	0.5	Fixture	12000
Weld	10min/part 8%, 2men	0.16	Welder	5000
QC	10min/part 8%, 2men	0.16	Fixture	3000
Paint	30min/part, 25%, 1 man	0.25	Paint Booth	7500
Support Hardware				
Shear & punch	10min/part, 8%, 1man	0.08	Shears & Punch (same)	
Fixture & weld	15min/part, 12%, 1man	0.12	Fix & welder	8000
Paint	6min/part,5%, 1man	0.05	Fixtures	2000
Assemble	6min/part,5%, 1man	0.05	Fixtures	2000
Front Membrane				
Laminate	5ft/min,10%, 3men	0.3	Laminator line	85000
Seam weld & trim	60min/part, 50%, 2men	1	Welder & fix	60000
			Mandrels (20)	10000
Rear Membrane				
Shear doublers	15min/part, 12%, 1 man	0.12	Power Shear	3000
Seam Weld & trim	60min/part, 50%, 2men	1	Welder & fix	60000
Install Doubler	15min/part, 12%, 1man	0.12	Fixture	2000
			Mandrels (20)	10000
Clips				
Slit	10ft/min,1%, 1 man	0.01	Uncoiler & Slitter	26000
Punch	6min/part, 5%,1man	0.05	Punch	10000
Roll Form	6min/part, 5%, 1 man	0.05	Roll former	30000
Assemble				
Fixture ring	10min/part, 8%, 2men	0.16	Fixture	80000
Install & clip rear mem	40min/part, 33%, 2men	0.67	Clip tool	50000
Install frnt memb	40min/part, 33%, 2men	0.67		
Form, QC, Clip	30min/part,.25,2men	0.5	QC Tooling	8000
Install flange & tether	10min/part, 8%, 1 man	0.08		
Install control interfa	10min/part, 8%, 1man	0.08	Fixture	1000
Mount on racks	15min/part, 12%, 2men	0.25		
Control box assy	90min/12, 3%, 1man	0.03	Fixture	2000
Misc				
			Forklift	15000
			Overhead trolley	20000
			Shipping racks	0
			Other	25000
	Sum	6.82		630500
	Hrs/part	13.64		

10000 Rate

@ 10,000 facets per year, 2000 hrs per year

(40 units per day)

Process	Rate	Men	Equipment	Equip $
Ring				
Roll & Shear Chanl	20ft/min 15% of time	0.15	Roll Former	75000
Punch holes	2min/part 15% of time	0.15	Punch station	9000
Bend & trim	4min/part 30%, 2 men	0.6	Roll bender	30000
Shear Doubler	.5min/part 5%	0.05	Shear	20000
Fixture & prep	8min/part 67%, 2 men	1.34	Fixture(2)	30000
Weld	4min/part 33%, 2 men	0.66	Welder	6000
QC	4min/part 33%, 2men	0.66	Fixture	5000
Paint	12min/part, 100%, 1 man	1	Paint Booth	25000
Support Hardware				
Shear & punch	2min/part, 50%, 1 man	0.5	Shears & Punch (same)	
Fixture & weld	3min/part, 75%, 1man	0.75	Fix & welder	10000
Paint	2min/part, 50%, 1man	0.5	Fixtures	3000
Assemble	1min/part, 25%, 1man	0.25	Fixtures	3000
Front Membrane				
Laminate	10ft/min,50%, 3men	1.5	Laminator line	100000
Seam weld & trim	0.4hr/part,200%,2men	4	Welder & fix(2)	140000
			Mandrels (40)	20000
Rear Membrane				
Shear doublers	5min/part 40% 1man	0.4	Power Shear	5000
Seam Weld & trim	0.4hr/part, 200%,2men	4	Welder & fix(2)	140000
Install Doubler	6min/part, 50% 1man	0.5	Fixture	5000
			Mandrels (40)	20000
Clips				
Slit	15ft/hr,3%,1man	0.03	Uncoiler & Slitter	26000
Punch	2min/part, 15%, 1man	0.15	Punch	15000
Roll Form	1min/part, 8%, 1man	0.08	Roll former	35000
Assemble				
Fixture ring	4min/part, 33%, 2men	0.67	Fixture & misc (4)	400000
Install & clip rear mem	12min/part, 100%, 2men	2	Clip tool	75000
Install frnt memb	12min/part, 100%, 2men	2		
Form, QC, Clip	12min/part, 100%, 2men	2	QC Tooling	12000
Install flange & tether	4min/part, 33%, 1man	0.33		
Install control interfa	4min/part, 33%, 1man	0.33	Fixture	2000
Mount on racks	12min/part, 100%, 1man	1		
Control box assy	60min/12, 42%, 1man	0.42	Fixture	3000
Misc				
			Forklifts (2)	30000
			Overhead trolley	40000
			Shipping racks	0
			Other	50000
	Sum	26.02		1334000
	Hrs/part	5.204		

APPENDIX C
COST ANALYSIS

Gross margin is defined as the gross revenue prior to taxes and depreciaton. Payable dividend is the gross margin less tax.

500 units/year
Cost analysis for commercial production of stretched membrane facets

MANUFACTURING EQUIPMENT	630500	$	YEAR 1 MATERIAL COST	422.71	$/UNIT
OFFICE EQUIPMENT	100000	$	MATERIAL OVERHEAD	0.10	% Mt'l Cost/100
TOTAL CAPITAL EXPENSE	730500		DIRECT MAN HOURS	13.64	/UNIT
ORGANIZATIONAL EXPENSE (nondeductable)	100000	$	DIRECT LABOR RATE	9.00	$/MH
TOTAL STARTUP COSTS	830500	$	LABOR BURDEN	0.70	% Drt Labor/100
DEPRECIATION	7	YEARS			
UNITS SOLD PER YEAR	500		R&D	0.03	% SALES/100
UNIT SALE PRICE	1156.8	$	G&A	0.35	%/100
INFLATION RATE	0.04	%/100	FED. TAX RATE	0.34	% Profit/100
DISCOUNT RATE	0.15	%/100	STATE TAX RATE	0.04	% Profit/100
EQUIPMENT RESALE FACTOR	0.10		FACET AREA	10.05	SQ M

YEAR	1	2	3	4	5	6	7	8	9	10	11
UNITS SOLD	500	500	500	500	500	500	500	500	500	500	0
SALE PRICE	1157	1203	1251	1301	1353	1407	1464	1522	1583	1646	0
GROSS SALES	578400	601536	625597	650621	676646	703712	731861	761135	791580	823244	108132
MATERIAL COSTS	211355	219809	228602	237746	247255	257146	267432	278129	289254	300824	0
MATERIAL O.H.	21136	21981	22860	23775	24726	25715	26743	27813	28925	30082	0
DIRECT LABOR	61380	63835	66389	69044	71806	74678	77665	80772	84003	87363	0
LABOR BURDEN	42966	44685	46472	48331	50264	52275	54366	56540	58802	61154	0
SHIPPING COSTS	0	0	0	0	0	0	0	0	0	0	0
R&D COSTS	17352	18046	18768	19519	20299	21111	21956	22834	23747	24697	0
G&A EXPENSE	42594	44298	46070	47913	49829	51822	53895	56051	58293	60625	0
GROSS MARGIN	181617	188882	196437	204295	212466	220965	229804	238996	248556	258498	108132
DEPRECIATION	104357	104357	104357	104357	104357	104357	104357	0	0	0	0
TAXABLE INCOME	77260	84525	92080	99938	108109	116608	125447	238996	248556	258498	108132
FED. INCOME TAX	26268	28738	31307	33979	36757	39647	42652	81259	84509	87889	36765
STATE INCOME TAX	3090	3381	3683	3998	4324	4664	5018	9560	9942	10340	4325
AFTER TAX PROFIT	47901	52405	57090	61961	67028	72297	77777	148177	154105	160269	67042
PROFIT AS % OF SALES	0.083	0.087	0.091	0.095	0.099	0.103	0.106	0.195	0.195	0.195	0.620
PAYABLE DIVIDEND	152258	156762	161447	166318	171385	176654	182134	148177	154105	160269	67042
830666 = PV =	132399	118535	106154	95093	85209	76372	68471	48439	43806	39616	16572
1st YR COST ($/SQm)=	115.10										

1000 units/year
Cost analysis for commercial production of stretched membrane facets

MANUFACTURING EQUIPMENT	630500	$	YEAR 1 MATERIAL COST	418.43	$/UNIT
OFFICE EQUIPMENT	100000	$	MATERIAL OVERHEAD	0.10	% Mt'l Cost/100
TOTAL CAPITAL EXPENSE	730500		DIRECT MAN HOURS	13.64	/UNIT
ORGANIZATIONAL EXPENSE (nondeductable)	100000	$	DIRECT LABOR RATE	9.00	$/MH
TOTAL STARTUP COSTS	830500	$	LABOR BURDEN	0.70	% Drt Labor/100
DEPRECIATION	7	YEARS			
UNITS SOLD PER YEAR	1000		R&D	0.03	% SALES/100
UNIT SALE PRICE	937.9	$	G&A	0.25	%/100
INFLATION RATE	0.04	%/100	FED. TAX RATE	0.34	% Profit/100
DISCOUNT RATE	0.15	%/100	STATE TAX RATE	0.04	% Profit/100
EQUIPMENT RESALE FACTOR	0.10		FACET AREA	10.05	SQ M

YEAR	1	2	3	4	5	6	7	8	9	10	11
UNITS SOLD	1000	1000	1000	1000	1000	1000	1000	1000	1000	1000	0
SALE PRICE	938	975	1014	1055	1097	1141	1187	1234	1284	1335	0
GROSS SALES	937900	975416	1014433	1055010	1097210	1141099	1186743	1234212	1283581	1334924	108132
MATERIAL COSTS	418430	435167	452574	470677	489504	509084	529447	550625	572650	595556	0
MATERIAL O.H.	41843	43517	45257	47068	48950	50908	52945	55063	57265	59556	0
DIRECT LABOR	122760	127670	132777	138088	143612	149356	155331	161544	168006	174726	0
LABOR BURDEN	85932	89369	92944	96662	100528	104549	108731	113081	117604	122308	0
SHIPPING COSTS	0	0	0	0	0	0	0	0	0	0	0
R&D COSTS	28137	29262	30433	31650	32916	34233	35602	37026	38507	40048	0
G&A EXPENSE	59207	61576	64039	66600	69264	72035	74916	77913	81029	84270	0
GROSS MARGIN	181591	188854	196409	204265	212435	220933	229770	238961	248519	258460	108132
DEPRECIATION	104357	104357	104357	104357	104357	104357	104357	0	0	0	0
TAXABLE INCOME	77234	84497	92051	99908	108078	116576	125413	238961	248519	258460	108132
FED. INCOME TAX	26259	28729	31297	33969	36747	39636	42640	81247	84497	87876	36765
STATE INCOME TAX	3089	3380	3682	3996	4323	4663	5017	9558	9941	10338	4325
AFTER TAX PROFIT	47885	52388	57072	61943	67009	72277	77756	148156	154082	160245	67042
PROFIT AS % OF SALES	0.051	0.054	0.056	0.059	0.061	0.063	0.066	0.120	0.120	0.120	0.620
PAYABLE DIVIDEND	152242	156745	161429	166300	171366	176634	182113	148156	154082	160245	67042
830571 = PV =	132384	118522	106142	95083	85199	76364	68463	48432	43800	39610	16572

1st YR COST ($/SQm)= 93.32

10,000 units/year
Cost analysis for commercial production of stretched membrane facets

MANUFACTURING EQUIPMENT	1334000	$	YEAR 1 MATERIAL COST	403.57	$/UNIT
OFFICE EQUIPMENT	100000	$	MATERIAL OVERHEAD	0.05	% Mt'l Cost/100
TOTAL CAPITAL EXPENSE	1434000		DIRECT MAN HOURS	5.20	/UNIT
ORGANIZATIONAL EXPENSE (nondeductable)	100000	$	DIRECT LABOR RATE	9.00	$/MH
TOTAL STARTUP COSTS	1534000	$	LABOR BURDEN	0.50	% Drt Labor/100
DEPRECIATION	7	YEARS			
UNITS SOLD PER YEAR	10000		R&D	0.03	% SALES/100
UNIT SALE PRICE	556.64	$	G&A	0.15	%/100
INFLATION RATE	0.04	%/100	FED. TAX RATE	0.34	% Profit/100
DISCOUNT RATE	0.15	%/100	STATE TAX RATE	0.04	% Profit/100
EQUIPMENT RESALE FACTOR	0.10		FACET AREA	10.05	SQ M

YEAR	1	2	3	4	5	6	7	8	9	10	11
UNITS SOLD	10000	10000	10000	10000	10000	10000	10000	10000	10000	10000	0
SALE PRICE	557	579	602	626	651	677	704	733	762	792	0
GROSS SALES	5566400	5789056	6020618	6261443	6511901	6772377	7043272	7325003	7618003	7922723	212267
MATERIAL COSTS	4035700	4197128	4365013	4539614	4721198	4910046	5106448	5310706	5523134	5744059	0
MATERIAL O.H.	201785	209856	218251	226981	236060	245502	255322	265535	276157	287203	0
DIRECT LABOR	468000	486720	506189	526436	547494	569394	592169	615856	640490	666110	0
LABOR BURDEN	234000	243360	253094	263218	273747	284697	296085	307928	320245	333055	0
SHIPPING COSTS	0	0	0	0	0	0	0	0	0	0	0
R&D COSTS	166992	173672	180619	187843	195357	203171	211298	219750	228540	237682	0
G&A EXPENSE	130349	135563	140985	146625	152490	158589	164933	171530	178391	185527	0
GROSS MARGIN	329574	342757	356467	370726	385555	400977	417017	433697	451045	469087	212267
DEPRECIATION	204857	204857	204857	204857	204857	204857	204857	0	0	0	0
TAXABLE INCOME	124717	137900	151610	165869	180698	196120	212159	433697	451045	469087	212267
FED. INCOME TAX	42404	46886	51548	56395	61437	66681	72134	147457	153355	159490	72171
STATE INCOME TAX	4989	5516	6064	6635	7228	7845	8486	17348	18042	18763	8491
AFTER TAX PROFIT	77325	85498	93998	102839	112033	121595	131539	268892	279648	290834	131606
PROFIT AS % OF SALES	0.014	0.015	0.016	0.016	0.017	0.018	0.019	0.037	0.037	0.037	0.620
PAYABLE DIVIDEND	282182	290355	298856	307696	316890	326452	336396	268892	279648	290834	131606
1534318 = PV =	245375	219550	196502	175926	157550	141134	126464	87901	79493	71890	32531

1st YR COST ($/SQm)= 55.39

UNLIMITED DISTRIBUTION
INITIAL DISTRIBUTION

U.S. Department of Energy (5)
Forrestal Building
Code CE-314
1000 Independence Avenue, SW
Washington, DC 20585
Attn: M. Scheve
S. Gronich

U.S. Department of Energy (2)
Forrestal Building
Code CE-33
1000 Independence Avenue, SW
Washington, DC 20585
Attn: B. Annan

U.S. Department of Energy (3)
Albuquerque Operations Office
P.O. Box 5400
Albuquerque, NM 87115
Attn: C. Garcia
G. Tennyson
N. Lackey

U.S. Department of Energy
San Francisco Operations Office
1333 Broadway
Oakland, CA 94612
Attn: R. Hughey

AAI Corporation
P. O. Box 6787
Baltimore, MD 21204

Acurex Corporation (2)
555 Clyde Avenue
Mountain View, CA 94039
Attn: J. Schaefer
H. Dehne

Advanced Thermal Systems
7600 East Arapahoe
Suite 319
Englewood, CO 80112
Attn: D. Gorman

Arizona Public Service Company
P.O. Box 21666
Phoenix, AZ 85036
Attn: J. McGuirk

Arizona Solar Energy Office
Dept. of Commerce
1700 W. Washington, 5th Floor
Phoenix, AZ 85007
Attn: F. Mancini

Australian National University
Department of Engineering Physics
P. O. Box 4
Canberra ACT 2600 AUSTRALIA
Attn: S. Kaneff

Barber-Nichols Engineering
6325 West 55th Avenue
Arvada, CO 80002
Attn: R. Barber

Battelle Pacific Northwest
Laboratory (2)
P.O. Box 999
Richland, WA 99352
Attn: T. A. Williams
D. Brown

BDM Coporation
1801 Randolph Street
Albuquerque, NM 87106
Attn: W. Schwinkendorf

Bechtel National, Inc.
50 Beale Street
50/15 D8
P. O. Box 3965
San Francisco, CA 94106
Attn: P. DeLaquil

Black & Veatch Consulting
Engineers
P.O. Box 8405
Kansas City, MO 64114
Attn: J. C. Grosskreutz

Tom Brumleve
1512 Northgate Road
Walnut Creek, CA 94598

California Energy Commission
1516 Ninth Street, M-S 43
Sacramento, CA 95814
Attn: A. Jenkins

California Polytechnic University
Dept. of Mechanical Engineering
Pomona, CA 91768
Attn: W. Stine

California Public Utilities Com.
Resource Branch, Room 5198
455 Golden Gate Avenue
San Francisco, CA 94102
Attn: T. Thompson

Cummins Engine Co.
MC 60125
P. O. Box 3005
Columbus, IN 47202-3005
Attn: R. Kubo

Dan Ka
3905 South Mariposa
Englewood, CO 80110
Attn: D. Sallis

DLR
Pfaffenwaldring 38-40
7000 Stuttgart 80 WEST GERMANY
Attn: R. Buck

DSET
P. O. Box 1850
Black Canyon Stage I
Phoenix, AZ 85029
Attn: G. Zerlaut

Electric Power Research
Institute
P.O. Box 10412
Palo Alto, CA 94303
Attn: J. Schaeffer

Engineering Perspectives
20 19th Avenue
San Francisco, CA 94121
Attn: John Doyle

Energy Technology Engr. Center
Rockwell International Corp.
P. O. Box 1449
Canoga Park, CA 91304
Attn: W. Bigelow

ENTECH, Inc.
P. O. Box 612246
DFW Airport, TX 75261
Attn: R. Walters

Florida Solar Energy Center
300 State Road 401
Cape Canaveral, FL 32920
Attn: Library

Ford Aerospace
Ford Road
Newport Beach, CA 92663
Attn: R. Babbe

Foster Wheeler Solar Development
Corporation (2)
12 Peach Tree Hill Road
Livingston, NJ 07039
Attn: M. Garber
R. Zoschak

Garrett Turbine Engine Co.
111 South 34th Street
P. O. Box 5217
Phoenix, AZ 85010
Attn: E. Strain

Georgia Power (2)
7 Solar Circle
Shenandoah, GA 30265
Attn: W. King

Harris Corporation (2)
Government and Aerospace
Systems Division
P. O. Box 9400
Melbourne, FL 32902
Attn: K. Schumacher

Industrial Solar Technologies
5775 West 52nd Avenue
Denver, CO 80212
Attn: R. Gee

Institute of Gas Technology
34245 State Street
Chicago, IL 60616
Attn: Library

ISEIR
951 Pershing Drive
Silver Spring, MD 20910
Attn: A. Frank

Jet Propulsion Laboratory
4800 Oak Grove Drive
Pasadena, CA 91109
Attn: M. Alper

LaJet Energy Company
P. O. Box 3599
Abilene, TX 79604
Attn: M. McGlaun

L'Garde, Inc. (2)
1555 Placentia Avenue
Newport Beach, CA 92663
Attn: M. Thomas
J. Williams

Lawrence Berkeley Laboratory
MS 90-2024
One Cyclotron Road
Berkeley, CA 94720
Attn: A. Hunt

Luz International (2)
924 Westwood Blvd.
Los Angeles, CA 90024
Attn: D. Kearney

3M-Energy Control Products (2)
207-1W 3M Center
St. Paul, MN 55144
Attn: R. Dahlen

Mechanical Technology, Inc. (2)
968 Albany Shaker Road
Latham, NY 12110
Attn: G. Dochat
J. Wagner

Meridian Corporation
4300 King Street
Alexandria, VA 22302
Attn: D. Kumar

NASA Lewis Research Center (4)
21000 Brook Park Road
Cleveland, OH 44135
Attn: R. Beremand 500-215
R. Evans 500-210
J. Savino 301-5
R. Corrigan 500-316

Nevada Power Co.
P. O. Box 230
Las Vegas, NV 89151
Attn: Mark Shank

Pacific Gas and Electric Company (2)
3400 Crow Canyon Road
San Ramon, CA 94526
Attn: G. Braun
J. Iannucci

Polydyne, Inc.
1900 S. Norfolk Street, Suite 209
San Mateo, CA 94403
Attn: P. Bos

Power Kinetics, Inc.
415 River Street
Troy, NY 12180
Attn: W. Rogers

Renewable Energy Institute
1001 Connecticut Ave. NW
Suite 719
Washington, DC 20036
Attn: K. Porter

Rocketdyne Division
6633 Canoga Park Ave.
Canoga Park, CA 91304
Attn: W. Marlatt

San Diego Gas and Electric Company
P.O. Box 1831
San Diego, CA 92112
Attn: R. Figueroa

SCE
P. O. Box 800
Rosemead, CA 91770
Attn: P. Skvarna

Schlaich, Bergermann & Partner
Hohenzollernstr. 1
D - 7000 Stuttgart 1
West Germany
Attn: W. Schiel

Sci-Tech International
Advanced Alternative Energy
Solutions
5673 W. Las Positas Boulevard
Suite 205
P.O. Box 5246
Pleasanton, CA 84566
Attn: U. Ortabasi

Science Applications International
Corporation (2)
10343 Roselle Street, Suite G
San Diego, CA 92121
Attn: K. Beninga

Solar Energy Research Institute (5)
1617 Cole Boulevard
Golden, CO 80401
Attn: B. Gupta
L. M. Murphy
G. Jorgensen
T. Wendelin
A. Lewandowski

Solar Kinetics, Inc. (2)
P.O. Box 540636
Dallas, TX 75354-0636
Attn: J. A. Hutchison
P. Schertz
D. Konnerth

Solar Power Engineering Company
P.O. Box 91
Morrison, CO 80465
Attn: H. Wroton

Solar Steam
P. O. Box 32
Fox Island, WA 98333
Attn: D. Wood

SPECO
P. O. Box 91
Morrison, CO 80465
Attn: W. Hart

SRS Technologies
990 Explorer Blvd., NW
Huntsville, AL 35806
Attn: R. Bradford

Stearns Catalytic Corporation
P.O. Box 5888
Denver, CO 80217
Attn: T. E. Olson

Stirling Thermal Motors
2841 Boardwalk
Ann Arbor, MI 48104
Attn: B. Ziph

Sun Power, Inc.
6 Byard Street
Athens, OH 45701
Attn: W. Beale

Tom Tracey
6922 South Adams Way
Littleton, CO 80122

United Solar Tech, Inc.
3434 Martin Way
Olympia, WA 98506
Attn: R. Kelley

University of Chicago
Enrico Fermi Institute
5640 Ellis Avenue
Chicago, IL 60637
Attn: J. O'Gallagher

University of Houston
Solar Energy Laboratory
4800 Calhoun
Houston, TX 77704
Attn: L. Vant-Hull

University of Utah
Mechanical and Industrial
Engineering
Salt Lake City, UT 84112
Attn: B. Boehm

Eric Weber
302 Caribbean Lane
Phoenix, AZ 85022

WG Associates
6607 Stonebrook Circle
Dallas, TX 75240
Attn: V. Goldberg

1840 R. E. Loehman
1846 D. H. Doughty
1846 C. S. Ashley

3141 S.A. Landenberger (5)
3151 G.C. Claycomb (3)
3145 Document Processing (8)
for DOE/OSTI

6000 V. L. Dugan, Actg.
6200 B. W. Marshall, Actg.
6210 J. T. Holmes, Actg.
6215 C. P. Cameron
6215 R. M. Houser
6216 C. E. Tyner
6216 L. Yellowhorse
6216 D. J. Alpert
6216 J. W. Grossman
6216 T. R. Mancini (30)
6216 J. E. Pacheco
6217 P. C. Klimas
6217 K. L. Linker
6217 R. B. Diver
6220 D. G. Schueler
6221 E. C. Boes
6223 G. J. Jones
6224 A. R. Mahoney
7470 J. L. Ledman
7476 F. P. Gerstle
7476 S. T. Reed
8523 R.C. Christman